International Journal of Biological Macromolecules 323 (2025) 147124

Contents lists available at ScienceDirect

International Journal of Biological Macromolecules

journal homepage: www.elsevier.com/locate/ijbiomac

Intelligent film based on collagen and anthocyanins from *Catharanthus roseus*: a new freshness sensor for fish

Gabrielle Ingrid Bizerra Florentino [a], Cristiani Viegas Brandão Grisi [b,*], Marcos dos Santos Lima [a], Rita de Cassia Andrade da Silva [b], Valquíria Cardoso da Silva Ferreira [c], Angela Maria Tribuzy de Magalhães Cordeiro [c], Fábio Anderson Pereira da Silva [a]

[a] *Post-Graduate Program in Food Science and Technology, Department of Food Engineering, Technology Center, Federal University of Paraíba, João Pessoa, Paraíba, Brazil*
[b] *Post-Graduate Program in Chemical, Department of Chemistry, Center for Exact and Natural Sciences, Federal University of Paraíba, João Pessoa, Paraíba, Brazil*
[c] *Post-Graduate Program in Agro-Food Technology, Center for Humans, Social and Agrarian Sciences, Federal University of Paraiba, Bananeiras, Paraiba, Brazil*

ARTICLE INFO

Keywords:
Intelligent packaging
Colorimetric sensor
Flower anthocyanin
Collagen film
Fish freshness

ABSTRACT

This study evaluated the impact of different concentrations of anthocyanin extract (CAE) from *Catharanthus roseus* flowers, an innovative and little-explored source of anthocyanins, on the properties of intelligent films for monitoring the freshness of tilapia fillets. The films were produced from collagen from tilapia skin and pectin, in 4 treatments: FC (control), F10 (10 % CAE), F20 (20 % CAE) and F30 (30 % CAE). The results demonstrated that CAE presented high anthocyanin content, significant antioxidant activity, and phenolic profile composed of phenolic acids, flavonoids and anthocyanins, in addition to color variation sensitive to changes in pH. The incorporation of CAE darkened the films and compromised the elasticity and thermal resistance at the highest concentrations (30 %), without affecting the tensile strength, solubility, and vapor permeability. The higher concentration of CAE also reduced soil film degradation, decreased crystallinity, and increased antioxidant activity. The films demonstrated sensitivity to the presence of different concentrations of ammonia, evidenced by chromatic changes. Among the treatments, the F30 film demonstrated a quick response to pH variations associated with fish spoilage, with a noticeable transition from translucent to an opaque yellowish. These results demonstrate the feasibility of using CAE in intelligent and sustainable systems for monitoring fish freshness.

1. Introduction

The increasing use of plastic products in everyday life has led to a massive accumulation of plastic waste in various ecosystems, such as microplastics, being a serious threat to aquatic environments and human health. These fragments are ingested by marine organisms, causing bioaccumulation of toxins and health risks through the food chain [1]. Detected in human tissues, such as the placenta, microplastics raise concerns about their long-term effects [2]. To combat this crisis, it is crucial to improve recycling processes and invest in biodegradable alternatives.

In this context, bioplastics present themselves as a promising alternative to traditional plastics, providing environmental benefits through their biodegradability and production from sustainable sources [3]. Among the innovative options, bioplastics made from fish collagen stand out, which use waste from the fishing industry to create biodegradable materials [4]. These bioplastics have good mechanical properties and flexibility and are especially suitable for food packaging. In addition to reducing environmental pollution, this approach promotes a zero-waste strategy [5].

In recent years, scientists have highlighted the potential of natural bioactive substances to improve the functional properties of films. Furthermore, in the field of food safety, there is a growing demand for solutions that track food quality during transportation and storage [6]. According to the World Health Organization (WHO), contaminated food is responsible for 600 million cases of foodborne illness and 420,000 deaths each year worldwide [7]. Intelligent food packaging has aroused great interest as they are systems that monitor internal and external

* Corresponding author.
E-mail address: crisgrisi.gere@gmail.com (C.V.B. Grisi).

https://doi.org/10.1016/j.ijbiomac.2025.147124
Received 13 June 2025; Received in revised form 8 August 2025; Accepted 24 August 2025
Available online 25 August 2025

changes in food, communicating these changes to the external environment, promoting traceability, transparency, and safety throughout the supply chain [8].

Among the promising technologies for these packaging, natural pigments sensitive to pH variations have been shown to be excellent colorimetric indicators, especially due to their ability to detect the accumulation of volatile amines, a process that occurs during the spoilage of protein-rich foods. These substances cause noticeable changes in the coloration of films containing pH-sensitive dyes [9]. In addition, indicators derived from natural sources offer advantages over chemically synthesized ones, mainly for food safety reasons and lower toxicity [10].

Among the most used natural pigments, anthocyanin, belonging to the group of polyphenols, stands out for its various biological activities, such as its potent antioxidant action. In addition to being an excellent alternative to synthetic dyes, due to its safety and biodegradability, anthocyanin also draws attention for its wide range of color variations, making it one of the most promising options for the development of intelligent packaging [11]. Previous studies have investigated different sources of anthocyanins, such as beets [12], red radish [13], apple peel [14], black rice [15], and rose [16], for the advancement of these technologies.

The development of freshness indicator films based on anthocyanins extracted from flowers is still limited. *Catharanthus roseus* (L.) Don., known as "bright eyes", is an ornamental plant native to Madagascar, with vibrant pink or white flowers. In addition to its aesthetic value, the plant has great medicinal importance, being a source of alkaloids used in chemotherapy [17]. Its flowers are rich in phenolic compounds, including flavonoids, anthocyanins, quercetin, and cinnamic acid derivatives, which enhances its use in various applications [18].

This study stands out for using, for the first time, anthocyanins from *Catharanthus roseus*, a plant widely cultivated and readily available in various tropical and subtropical regions, facilitating access and obtaining the material for extraction. Furthermore, this species exhibits intense coloration in its petals, a characteristic that indicates a high concentration and diversity of flavonoid pigments, including anthocyanins. Its phytochemical composition has been studied and recognized for its pharmacological properties, suggesting that its anthocyanins may have interesting functional characteristics, such as high antioxidant activity, enhancing their use in industrial and food applications. This approach leverages underutilized natural resources in the visual detection of food freshness. Thus, incorporating these anthocyanins into films based on tilapia skin collagen demonstrates the potential to indicate the freshness of tilapia fillets, expanding their applications in monitoring food quality.

2. Material and methods

2.1. Material

The flowers of *Catharanthus roseus* were collected manually at the Federal University of Paraíba (UFPB), Paraiba, Brazil, between June and September 2024, at the maximum stage of flowering and lilac coloration, and transported to NPE-LACOM/UFPB. The tilapia skin and fillet were purchased at the local market in João Pessoa, Paraíba State, Brazil, at refrigeration temperature (5 °C). The reagents used, such as glycerol, citrus pectin, citric acid, ethyl alcohol and buffer solutions, were supplied by the companies Dinâmica, Sheron, Alphatec and Labsynth, respectively, with analytical grade purity.

2.2. Obtaining Tilapia skin collagen (TSC)

Collagen extraction followed the method of Costa et al. [19]. The tilapia skin was washed, homogenized with water (1:1), heated to 60 °C for 1 h, and filtered through a stainless-steel sieve (18 cm in diameter, model SQ3701). The solution obtained was frozen at −18 °C for 24 h, cooled at 5 °C for 48 h for water drainage, and the resulting mass was frozen at −46 °C and lyophilized (Liotp L101) for 48 h. The samples were vacuum-packed and stored under freezing until use.

2.2.1. Extraction yield, chemical and physical characterization of collagen

The collagen extraction yield was calculated by the ratio of the weight of the lyophilized collagen to the wet weight of the skin. The quantification of collagen in the TSC was performed by the hydroxyproline method, in triplicate [20], where the sample was hydrolyzed with sulfuric acid, filtered and diluted. Hydroxyproline was oxidized with chloramine T, generating purple-red color. The intensity of the color was measured at 558 nm in a UV-VIS spectrophotometer (Shimadzu UV-2550) to determine the collagen concentration, according to Eqs. (1) and (2):

$$\mathrm{H(g/100\ g)} = \frac{(\mathrm{h\ x\ 2.5})}{(\mathrm{w\ x\ d})} \tag{1}$$

$$\mathrm{Collagenous\ tissue\ (g/100\ g)} = \mathrm{H} \times 8 \tag{2}$$

where: H = hydroxyproline. h = amount of hydroxyproline (μg) obtained from the standard curve. w = weight of the sample (g). d = dilution of the filtrate.

The analysis of the functional groups by Fourier Transform Infrared (FT-IR) was performed in a Shimadzu IR Prestige-2 spectrophotometer with ATR. The TSC was placed in the reading cell at 25 °C, and the spectra were collected from 600 to 4000 cm^{-1}, with a resolution of 4 cm^{-1} and 40 scans. After baseline correction, the self-deconvolution spectra were generated with IR Solutions software and adjusted in OriginPro.

2.3. Anthocyanin extraction from the Catharanthus roseus flower (CAE)

Preliminary tests were conducted with dried and fresh *Catharanthus roseus* flowers, using different solvents (water, ethanol, and acetic acid), to determine the most efficient extraction method for anthocyanins. Based on the results, fresh flowers and 75 % ethanol were chosen as the extraction solvent. Fresh flowers of *Catharanthus roseus* were macerated in 75 % ethanol solution (1:5, mass/volume) and kept at rest for 24 h at 5 °C, in a dark environment. After extraction, the solution was filtered and concentrated in a rotary evaporator (TECNAL, model TE-213) at 50 °C, until the ethanol was completely removed. The resulting extract was stored in an opaque glass container sealed with aluminum foil at 5 °C [21].

2.3.1. Physical, chemical and functional characterization of anthocyanin extract

The total solids content of CAE was obtained by the drying method in an oven at 105 °C, up to constant weight, in triplicate. Instrumental color was measured using a Konica Minolta digital colorimeter (CR-300), recording the parameters L*, a* and b*, in ten points, with calibration done with a standard white calibration plate, according to the specifications of the CIE [22].

The Total Anthocyanin Content (TAC) was analyzed by the differential pH method of Jeyaraj, Lim and Choo [23], in triplicate. The total anthocyanin content (TAC) of the extract was also monitored over 40 days, under storage in amber bottles at 5 °C. The absorbance of the samples was recorded in buffers pH 1 (potassium chloride 0.025 M) and pH 4.5 (sodium acetate 0.4 M) at wavelengths of 520 nm and 700 nm, using a UV-VIS spectrophotometer. The anthocyanin concentration was expressed in mg of cyanidin-3-glucoside equivalents/g of dry weight of extract (mg CGE/g extract). Absorbance was determined first, followed by quantification of total anthocyanins, according to Eqs. 3 and 4.

$$\mathrm{A} = (A_{520nm} - A_{700nm})pH1 - ((A_{520nm} - A_{700nm})pH4,5 \tag{3}$$

$$\mathit{Total\ Anthocyanin}\left(\frac{mg}{mL}\right) = \frac{A \times mm \times df \times 5}{\varepsilon \times 1} \tag{4}$$

where: A = absorbance; mm = molecular mass (449.2 g/mol); df = dilution factor; 1 = optical path length (cm); ε = 26,900, molar extinction coefficient (L/mol.cm) for cyanidin-3-glucoside; 5 = mandatory dilution of the method (1 mL of sample + 4 mL of buffer).

The antioxidant potential of CAE was evaluated by the ABTS and FRAP methods, in triplicate. In the ABTS method, 30 μL of the sample was mixed with 3.0 mL of ABTS solution, and the absorbance was measured at 734 nm after 30 min, with the results expressed in μmol of Trolox equivalent (TEAC) per gram of dry sample [24]. In the FRAP method, 10 μL of the extract was mixed with FRAP reagent and incubated at 37 °C for 30 min, with absorbance measured at 593 nm, and the results were also expressed in μmol of TEAC per gram of dry extract [25].

The identification of phenolic compounds was performed by an Agilent 1260 LC liquid chromatograph (Santa Clara, USA), equipped with a quaternary pump and in-line degasser (G1311C), thermostated column compartment (G1316A), autosampler (G1329B) and diode array detector (DAD, G1315D). Data collection and processing were performed using OpenLAB CDS ChemStation Edition software (Agilent Technologies, Santa Clara, USA). The column used was an Eclipse Plus RRHT RP-C18 (50 × 4.6 mm, 1.8 μm; Zorbax, SC, USA). The mobile phase consisted of 0.5 % *v*/v phosphoric acid (solvent A) and methanol acidified with 0.5 % v/v phosphoric acid (solvent B), with a flow rate of 1.0 mL/min at 40 °C, injecting 10 μL of the sample. The gradient was: 0 min: 0 % B; 2 min: 10 % B; 13 min: 26 % B; 19 min: 50 % B; 21 min: 80 % B; 21.1–23.1 min: 100 % B; 23.2 min: 0 % B, with 3 min of reequilibration. Phenolic detections occurred in the DAD at 220, 280, 320, 360, and 520 nm. The identification and quantification of the compounds were performed by comparison with external standards, considering retention time, calibration curves and spectral similarity [26].

The pH sensitivity of the CAE solution (1 mL extract: 1 mL buffer solution) was determined using a UV–Vis spectrophotometer (G105 UV–vis, Thermo Scientific Inc., USA). The solution spectra (pH 2.0–11.0) in the range of 400–800 nm was recorded and imaged to capture the colors of the solution.

2.4. Development of the films

The packages were prepared using the casting technique, according to the methodology adapted from Costa et al. [19], with a formulation of 2 % pectin, 2 % collagen and 1 % glycerol (*w*/w). The concentrations were defined based on preliminary tests, aiming at adequate film formation, good mechanical properties, and minimum use of ingredients. The pectin was dispersed in distilled water (25 °C), homogenized and left to rest for 24 h to hydrate. The collagen was dispersed in water with the pH adjusted to the range of 3 to 4 using 30 % citric acid. The collagen solution was heated to 83 °C in a microwave oven (SHARP - 342, Osaka, Japan), with continuous temperature monitoring using a digital thermometer (Ecotools - ET1415, Brazil). After heating, the hydrated pectin solution was incorporated into the collagen solution, homogenized and kept at 50 °C in a microwave oven for 3 min. The mixture was cooled to 40 °C, and the anthocyanin extract was added at concentrations of 10 %, 20 % and 30 % m/m and mechanical homogenizer for 5 min. The proportions refer to the mass of the concentrated extract in relation to the total mass of the film-forming matrix. Furthermore, the percentage was defined based on preliminary tests to ensure the color and functionality of the intelligent film. Concentrations above 30 % of the extract compromised the formation and applicability of the film. The solution was poured into sterile petri dishes (140 × 15 mm) and dried in an oven at 50 °C for about 15 h. After drying, the films were removed from the plates and subjected to analysis under environmental conditions of 25 °C and relative humidity of 60–70 %. The entire experiment was performed in a dark place to preserve the anthocyanin from exposure to sunlight.

2.4.1. Characterization of the physical, structural and morphological properties of films

The thickness of the bioplastic was measured with a portable micrometer (accuracy of 0.001 mm) at ten random points, 60 mm from the edges. The mean was used to evaluate the mechanical properties. The color was determined according to section 2.3.1, and the total color difference (ΔE) was calculated by Eq. 5, based on the difference between the parameters ΔL*, Δa* and Δb* of the control and the formulations. The colors of the films were also analyzed after 40 days of storage at 25 °C.

$$\Delta E^* = \left[(\Delta L^*)^2 + (\Delta a^*)^2 + (\Delta b^*)^2 \right]^{1/2} \quad (5)$$

Optical transmittance was evaluated in rectangular samples (10 × 40 mm) at 600 nm, using a UV–vis spectrophotometer (G105 UV–vis, Thermo Scientific), in triplicate. Transparency was calculated based on the transmittance obtained by the equation:

$$\text{Transparency} = -\log T600/x \quad (6)$$

where: T600 is the transmittance (%) at 600 nm, and x is the film thickness (mm).

The structural properties of the films, including tensile strength and elongation at break, were evaluated with a static analyzer (SHIMADZU) according to ASTM D882–12 [27]. Rectangular films (100 mm × 15 mm) were analyzed in ten replicates. The initial position of the jaws was 50 mm, with a separation speed of 12.5 mm/min. The results were expressed in MPa for tensile strength and as a percentage for elongation.

Solubility was determined according to Ojagh et al. [28], with modifications. 2 × 2 cm films were dried at 105 °C for 24 h, placed in 30 mL of distilled water at 25 °C and stirred for 24 h, in triplicate. After new drying, the final weight was recorded and the solubility calculated, according to eq. 7:

$$\text{Solubility (\%)} = [(\text{mi} - \text{mf})/\text{mi}] \text{ x } 100 \quad (7)$$

where: mi = the initial mass of the dry material (g) and mf = the final mass that has not dissolved (g).

Water vapor permeability (WVP) was evaluated by the gravimetric method (ASTM E96/E96M-16) [29]. Film samples were fixed inside a properly sealed container (3 cm in diameter) containing 10 g of silica gel, stored in a desiccator at 25 °C and 75 % relative humidity, and weighed every 24 h for 7 days, in triplicate. The WVP was calculated by the equation:

$$WVP = \frac{\left(\frac{C_i}{A}\right).X}{P_S.(RH_1 - RH_2)} \quad (8)$$

where: WVP = water vapor permeability, Ci = slope of the line generated by the weight loss of the system as a function of time, A = exposed surface area of the film (m^2), X = average film thickness, Ps = water saturation pressure, RH_1 = relative humidity inside the desiccator (75 %) and RH_2 = relative humidity inside the capsule (0 %). The results were expressed in g/m s Pa.

The degradability of the films was evaluated by the loss of mass after 60 days of exposure to soil. Rectangular samples (2 × 2 cm) were weighed, buried at 15 cm depth, and retrieved at intervals of 7, 15, 30, and 60 days. The films were washed with distilled water, dried at 50 °C for 24 h and weighed, in triplicate [30]. The percentage of degradation was then calculated using the following equation:

$$\text{Degradability (\%)} = [(\text{mi–mf})/\text{mi}] \text{ x } 100 \quad (9)$$

where: mi is the initial mass of the film (g), and mf is the final mass of the dry film (g).

X-ray diffraction (XRD) was performed on the XRD-6000 diffractometer (Shimadzu), with CuKα radiation (λ = 1.5418 Å), voltage of 30 kV and current of 30 mA, scanning angles from 10° to 50° at 2°/min, and the data were analyzed using the OriginPro 8.5 software [93]. The analysis to determine the functional groups of the films were performed by FT-IR, according to the procedure described in section 2.2.1.

The morphology of the films was analyzed by Scanning Electron Microscopy (SEM) under the MIRA-3 LMH microscope, with samples fixed on metal support, covered with gold. The images were acquired with 10 kV acceleration, using secondary electron (SE) detectors, 1750 mA flux and 5000× magnification.

The thermal analyses of the films (thermogravimetric analysis -TG/DTG and differential scanning calorimetry -DSC) (TG/DTG/DSC) were obtained with a simultaneous thermal analyzer SHIMADZU DTG—60H, using a sample of 5–10 mg, heated from 30 to 800 °C at 10 °C/min, in a nitrogen atmosphere (50 mL/min). The thermograms were processed in the OriginPro 8.5 software.

To evaluate the antioxidant potential of the films (FRAP and ABTS), the films were cut into 0.1 cm^2 squares (225 mg), dissolved in 10 mL of distilled water and stirred for 4 h. The solution was centrifuged at 3500 G for 12 min and the supernatant was used in the analyses, in triplicate. The methods employed are detailed in section 2.2.1.

2.4.2. Characterization of the functional properties of the films

The sensitivity of the films to detect ammonia vapors was tested according to Mei et al. [31]. Film samples with a diameter of 3.5 cm were exposed to flasks containing 10 mL of ammonium hydroxide solutions (10 % to 60 %) and films with 40 days of storage were exposed to 10 % ammonium hydroxide. The color change was recorded after 5 min of exposure, and the values L*, a* and b* were obtained with a colorimeter, in triplicate. The ΔE was calculated based on the color difference between each formulation and the film exposed to the solutions. For the stability test, the color difference of the films was determined based on the values obtained after 40 days of storage and exposure to the solutions.

2.5. Application of the films in the detection of freshness of tilapia fish

To evaluate the packaging as quality indicators, sterile jars of 70 mL and 5 cm in diameter were used, with tilapia fillet. The center of the lids has been removed, leaving only the snap-on part. Each jar received 20 g of fillet, with 3 cm of free space, and was closed with the corresponding packaging (F10, F20 and F30). The fillets were stored at 25 °C and relative humidity of 70 ± 5 %, to accelerate deterioration and evaluate the behavior of the intelligent packaging [32]. The samples were analyzed every 24 h for 72 h, in triplicate, for the difference in the color of the package and the pH of the fillet.

2.6. Statistical analysis

Data were analyzed using ANOVA ($p < 0.05$) and presented as mean ± standard deviation (SD). Significant differences between treatments were compared using Tukey's test (95 % confidence interval) using IBM-SPSS software, version 23.0. The charts were generated in Microsoft Excel 2023 or OriginPro, version 8.5 (OriginLab Corporation).

3. Results and discussion

3.1. Extraction yield, chemical and physical characterization of collagen

The yield of collagen extraction from tilapia skin was 6.31 % (Table 1) in relation to the wet weight of the skin. This is an intermediate value when compared to literature. Bi et al. [33], using hot water extraction, a method similar to the one used in this study, obtained a higher yield (10.7 %). On the other hand, different methodologies showed lower yields, as observed by Abdelaal et al. [34] with acid extraction (4.30 %) and Song et al. [35] using fermentation processes combined with chemical treatments (4.27–8.14 %). Considering that hot water extraction represents an economically viable and operationally simple approach, the yield obtained is satisfactory, although there is potential for optimization.

Table 1
Results of collagen and anthocyanin extract properties.

Bioactives	Parameters	Results
Collagen	Yield (%)	6.31 ± 0.0260
	Hydroxyproline (g/100 g)	4.83 ± 0.0240
	Collagenous tissue (g/100 g)	38.65 ± 0.190
Extract CAE	Total solids (g/mL)	0.047 ± 0.001
	TAC (mg/g)	4.780 ± 0.013
	TAC 40 day (mg/g)	2.358 ± 0.012
	L	33.875 ± 0.064
	a*	6.185 ± 0.078
	b*	−3.835 ± 0.035
	FRAP *(μmol trolox/g)*	383.620 ± 9.364
	ABTS *(μmol trolox/g)*	357.190 ± 25.610

Note: CAE (Anthocyanin Extraction from the *Catharanthus roseus*); TAC (Total Anthocyanin Content).

The quantification of hydroxyproline, the predominant amino acid in the collagen molecule, resulted in 4.83 g/100 g (Table 1). This value is close to the results reported by Song et al. [35], who observed 4.97 g/100 g when extracting collagen from tilapia skin by acid extraction, but is lower than the results obtained by Menezes et al. [36] who optimized the extraction conditions with different temperatures and acid treatments, reaching values between 6.81 and 6.94 g/100 g. The variations in hydroxyproline levels can be attributed both to environmental factors intrinsic to the raw material, especially the temperature of the fish habitat, and to the different extraction methodologies employed. Although the hydroxyproline found is consistent with the literature, the potential for optimization of extraction conditions is evidenced.

The FTIR spectra of collagen extracted from tilapia skin (Fig. 1-B) showed well-defined absorption bands at 3404 cm^{-1} (amide A), 3292 cm^{-1} (N—H stretch vibrations), 2924 cm^{-1} (amide B). In addition, the typical bands of amides I, II, and III were identified at 1629, 1546, and 1242 cm^{-1}, respectively [37]. This spectral profile is consistent with the results found by Elbialy et al. [38] and Reátegui-Pinedo et al. [39] for fish collagen, confirming the preservation of the typical triple helix structure and the presence of N—H groups involved in hydrogen bonding.

3.2. Chemical, physical and functional characterization of anthocyanin extract

The anthocyanin extract of the *Catharanthus roseus* flower showed instrumental color values L* (33.88), a* (6.19) and b* (−3.84), as shown in Table 1. The L* value indicates a low luminosity, reflecting a lower light transmittance and higher color intensity, characteristic of extracts with high chromatic density. The values of a* and b* suggest a moderate trend towards reddish tones and a predominance of bluish tones, respectively, corroborating the violaceous-blue coloration visually observed in the extract [11].

The total anthocyanin content of *Catharanthus roseus* extract (4.78 mg CGE/g) was higher than several floral extracts reported in the literature (Table 1). The observed concentration is higher than the content found in Hibiscus (0.266 mg CGE/g) [40], and close to the values obtained by Lin et al. [41] in *Aronia melanocarpa* (4.456 mg CGE/g) using eutectic solvents, being higher than the ultrasonic microwave-assisted ethanol extraction (2.996 mg CGE/g). Although lower than the anthocyanin content reported for *Clitoria ternatea* extracts (9.91 mg CGE/g) [42], the results highlight the potential of *Catharanthus roseus* as a promising source of anthocyanins.

The extract of *Catharanthus roseus* flowers showed a reduction in total anthocyanin (TAC) content from 4.57 mg CGE/g to 2.36 mg CGE/g

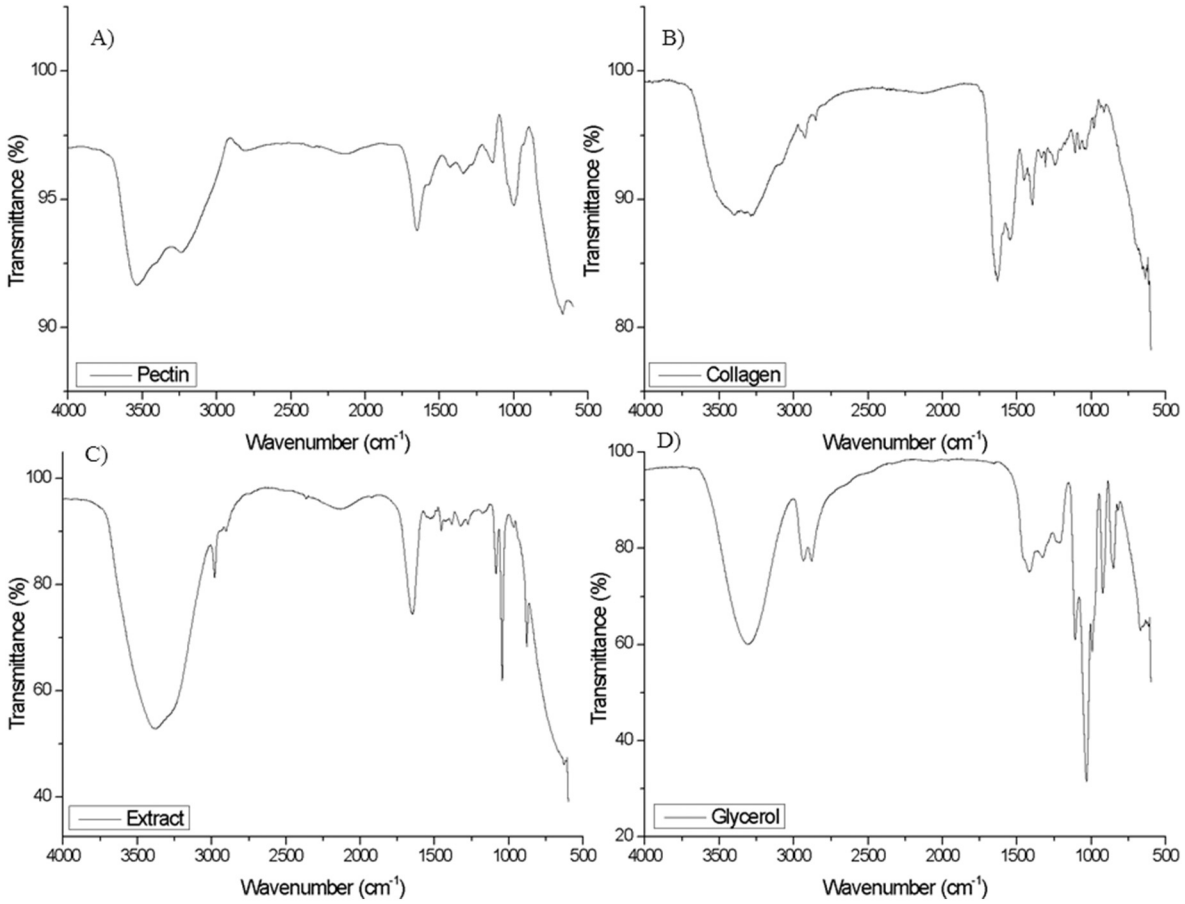

Fig. 1. FT-IR spectra A) Pectin; B) Collagen; C) Extract; D) Glycel; E) films added with CAE at different concentrations; F) Films degraded 60 days. FC: control; F10: 10 of CAE; F20: 20 of CAE; F30: 30 of CAE.

after 40 days under refrigeration, representing a retention of approximately 52 %. This result is comparable to that observed in other studies with non-encapsulated floral extracts, such *Delonix regia*, which showed a 55 % decrease in TAC after 35 days under similar conditions [43]. Although the stability of *Clitoria ternatea* L. extracts is generally superior, studies such as that of Zaidan et al. [44] demonstrate that, in the absence of encapsulation, even this extract can present losses of up to 40 % in 45 days depending on pH and temperature.

The antioxidant activity of CAE anthocyanin extract, evaluated by the ABTS and FRAP methods, showed significant results. The ABTS analysis resulted in 89.40 mg trolox/g (357.19 μmol trolox/g) (Table 1), higher than the *Clitoria ternatea* extracts obtained by reflux (52.48 mg trolox/g), but lower than those obtained by maceration (181.40 mg trolox/g) [45]. Similar results were observed by Baştürk and Yavaş, [46] in propolis (262.0 μmol trolox/g). The FRAP test showed values of 93.29 mg trolox/g (383.64 μmol trolox/g), values higher than those reported by Santos et al. [45] for *Clitoria ternatea* extracts obtained by maceration (112.10 μmol TEAC/g) and reflux (64.05 μmol TEAC/g). This variability highlights the influence of the plant matrix, extraction method and analytical technique used. The chemical structure of anthocyanins, including the glycosylated B-ring, enhances their antioxidant activity [47].

Analysis of the phenolic profile of *Catharanthus roseus* extract revealed 30 distinct metabolites, including phenolic acids (7), flavonoids (9), stilbenes (2), catechins (4), proanthocyanidins (3), phenolic aldehyde (1), and anthocyanins (4) (Table 2) (Fig. S1). Chlorogenic acid stood out as the main phenolic acid (2.938 g/kg), which is recognized for enhancing the stability and intensity of anthocyanin color, as demonstrated with extracts of Aronia [48] and other plant sources [49].

Among the flavonoids identified, hesperidin (15.679 g/kg), kaempferol 3-glucoside (9.583 g/kg) and isorhamnetin (5.667 g/kg) stood out. Hesperidin has antioxidant, anti-inflammatory, and antimicrobial properties, fighting oxidative stress related to chronic diseases [50], while kaempferol 3-glucoside, present in flowers such as *Asclepias syriaca* contributes to the stability of anthocyanins, as observed in extracts of *Hibiscus sabdariffa* [51]. Isorhamnetin, also isolated from *Asclepias syriaca*, enhances the antioxidant properties of the extract [52].

The cis-resveratrol (2.579 g/kg) and t-resveratrol (1.052 g/kg) stilbenes identified in the CAE extract, are known for their antioxidant, anti-inflammatory, and cardioprotective properties [53]. The main catechin identified was epigallocatechin gallate (EGCG) (2.522 g/kg), which inhibits peroxidase, preventing degradation and intensifying anthocyanin color [54]. The procyanidins B1, B2 and A2, identified in the extract, are important for the formation and stability of anthocyanins in hot and acidic environments [55], also present in flower buds of *Zingiber mioga* [56].

The anthocyanin profiles identified in the CAE included cyanidin 3-glucoside (0.052 g/kg), pelargonidin 3-glucoside (0.607 g/kg), peonidin 3-glucoside (0.098 g/kg), and malvidin 3-glucoside (0.516 g/kg), each with distinct roles in flower coloration. Cyanidin 3-glucoside, common in several plants, is sensitive to pH and metallic interactions [57], while pelargonidin 3-glucoside, predominant in red and orange flowers, interacts with carotenoids for chromatic modulation [58]. Peonidin 3-glucoside, associated with red and purple flowers [59], has greater stability due to glycosylation [60] and malvidin 3-glucoside, with a higher concentration in CAE, intensifies the color and increases the

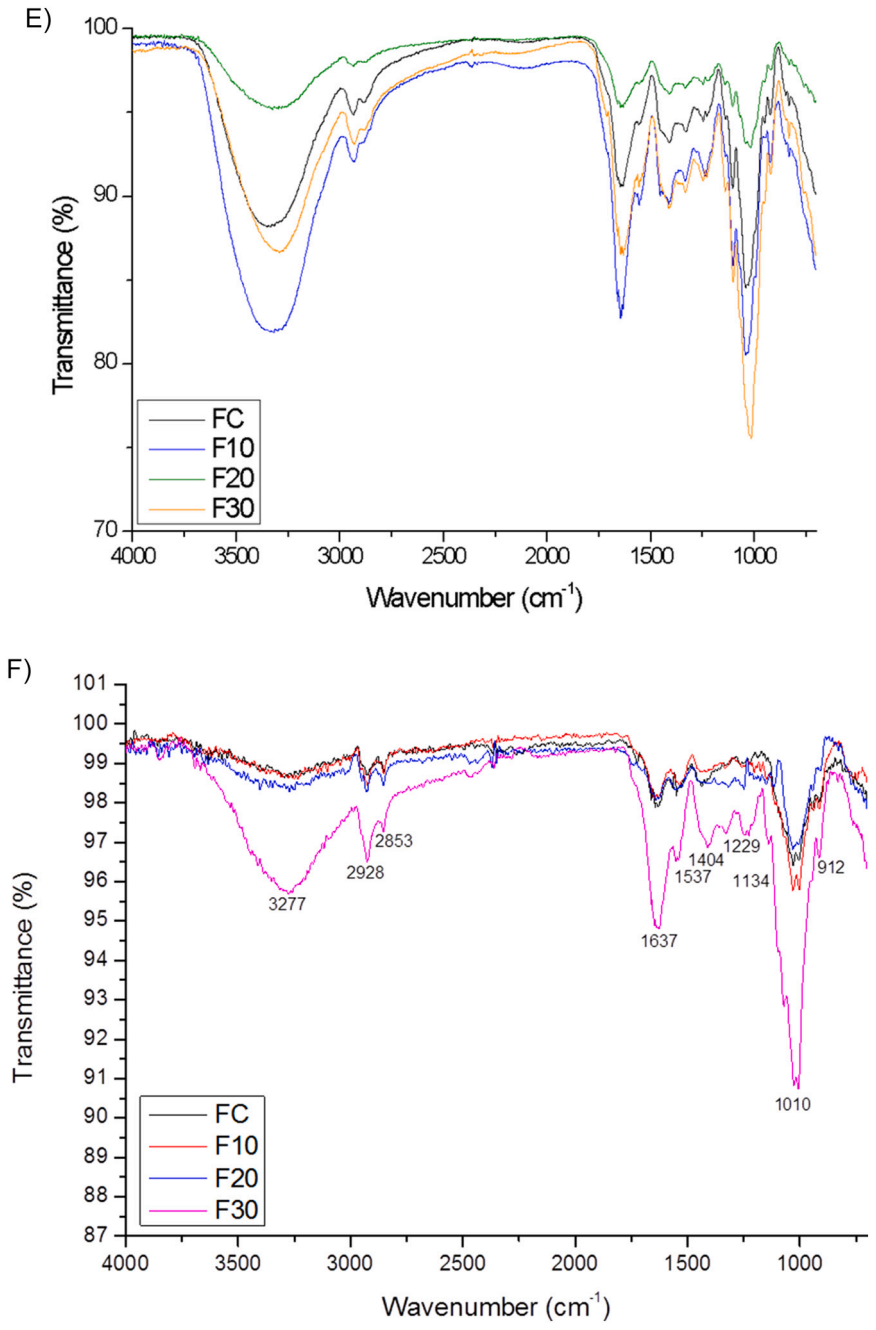

Fig. 1. (*continued*).

stability of flavanols, [61]. The pH-sensitive behavior of anthocyanins in CAE, coupled with its anthocyanin profile, makes the extract promising for application in intelligent films.

Spectroscopic analysis of the extract, subjected to different pH conditions (2−12), revealed a complex and gradual chromatic variation, as illustrated in Fig. 2A and B. The maximum absorption peak was recorded at approximately 542 nm, between pH 1 and 3, indicating the predominance of the flavylium cation, responsible for the red coloration, whose concentration decreased progressively with increasing pH [62]. Additionally, absorption peaks were observed at 564 nm (pH 5) and 598 nm (pH 12), accompanied by a gradual transition from violet to gray and, subsequently, to greenish tones. Similar results were reported by Li et al. [9] and Zhang et al. [63].

This behavior results from the typical structural changes of anthocyanins in response to pH variation (Fig. S2). Under highly acidic conditions (pH 1–3), the predominant species is the flavylium cation, characterized by a highly conjugated system involving the 2-phenylbenzopyrylium core and phenolic hydroxyl groups. This extended conjugation facilitates absorption in the visible region, resulting in an intense red coloration. As the pH increases to the range of 4–5, nucleophilic hydration of the flavylium ion occurs, leading to the formation of the carbinol base, an unstable and colorless intermediate. Simultaneously, proton transfer and tautomeric equilibria give rise to neutral structures known as quinoidal bases, which display violet hues typically observed at pH 6–7. In mildly alkaline environments (pH 7–9), further deprotonation of the quinoidal forms leads to the generation of anionic species, exhibiting purplish to bluish colors due to shifts in electron density and reorganization of the π-conjugated system. These structural modifications are governed by the dynamic keto-enol equilibrium characteristic of anthocyanins. At strongly alkaline pH values (≥ 9), ring opening of

Table 2
Identification of phenolic compounds from anthocyanin extract of *Catharanthus roseus* flower.

Phenolic compounds	Retention time (min)	λ (nm)	Amount (g/kg)
Phenolic acids			
Vanillic acid	6.488 ± 0.001	280	0.024 ± 0.000
Syringic acid	8.130 ± 0.003	280	0.045 ± 0.001
t-Cinnamic acid	17.755 ± 0.224	280	0.484 ± 0.128
Fumaric acid	1.489 ± 0.008	220	0.023 ± 0.000
p-Coumaric acid	9.407 ± 0.016	320	0.120 ± 0.006
Chlorogenic acid	6.929 ± 0.041	320	2.938 ± 0.129
Ferulic acid	11.370 ± 0.013	320	0.071 ± 0.004
Flavonoids			
Naringin	16.525 ± 0.001	280	1.717 ± 0.040
Hesperidin	17.348 ± 0.035	280	15.679 ± 0.568
Naringenin	19.170 ± 0.006	280	0.180 ± 0.075
Hesperitin	19.816 ± 0.004	280	0.117 ± 0.008
Myricetin	14.191 ± 0.052	360	2.290 ± 0.045
Quercetin 3-glucoside	16.300 ± 0.001	360	0.634 ± 0.047
Rutin	16.513 ± 0.002	360	0.513 ± 0.034
Kaempferol 3-glucoside	17.933 ± 0.028	360	9.583 ± 0.870
Isorhamnetin	18.183 ± 0.001	360	5.667 ± 0.125
Stilbenes			
cis-Resveratrol	17.952 ± 0.001	280	2.579 ± 0.242
t-Resveratrol	16.130 ± 0.001	320	1.052 ± 0.075
Catechins			
Epigallocatechin gallate	5.357 ± 0.001	220	2.522 ± 0.126
Catechin	5.746 ± 0.000	220	0.014 ± 0.001
Epicatechin	8.871 ± 0.010	220	0.138 ± 0.003
Epicatechin gallate	11.938 ± 0.019	220	0.033 ± 0.000
Proanthocyanidins			
Procyanidin B1	5.069 ± 0.000	220	0.017 ± 0.000
Procyanidin B2	7.209 ± 0.001	220	0.197 ± 0.008
Procyanidin A2	12.892 ± 0.007	220	0.785 ± 0.012
Phenolic aldehyde			
Vanillin	7.835 ± 0.000	320	0.019 ± 0.000
Anthocyanin			
Cyanidin 3-glucoside	11.603 ± 0.000	520	0.052 ± 0.003
Pelargonidin 3-glucoside	12.747 ± 0.018	520	0.607 ± 0.005
Peonidin 3-glucoside	14.059 ± 0.007	520	0.098 ± 0.000
Malvidin 3-glucoside	15.168 ± 0.008	520	0.516 ± 0.001

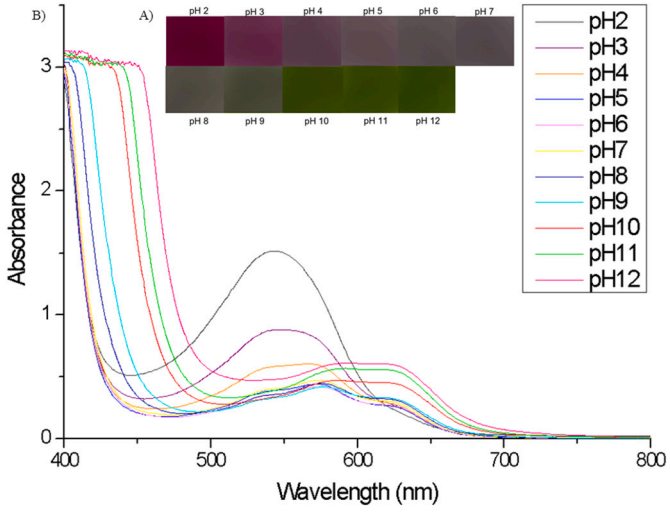

Fig. 2. A) Color changes of CAE in different buffer solutions ranging from pH 2 to 12, B) Ultraviolet–visible spectra of CAE in different buffer solutions ranging from pH 2 to 12.

the flavylium cation occurs, resulting in the formation of chalcone structures that impart a yellow coloration to the solution [64,65].

Under such conditions, however, chalcone degradation products have also been associated with the emergence of a green coloration, which may result from the overlap of bluish tones from anionic quinoidal forms and the yellow hue of chalcones, reflecting additional structural breakdown of anthocyanins in highly alkaline environments [66]. All these structural transitions are largely reversible, which gives anthocyanins high sensitivity and versatility as pH-dependent colorimetric indicators [67]. These characteristics make the anthocyanins from *Catharanthus roseus* promising for applications in intelligent films sensitive to food spoilage, especially due to their ability to reflect chemical changes associated with rancidity.

In addition to its experimentally observed function as a pH indicator, the ethanolic extract of *Catharanthus roseus* flowers demonstrated a safe toxicological profile. In an acute toxicity study, Nayak and Pinto [68] reported that oral administration of doses up to 8 g/kg to Sprague Dawley rats did not cause signs of toxicity or mortality. In contrast, the leaf extract of the same plant showed adverse effects starting at 300 mg/kg, as demonstrated by Vutukuri et al. [69]. These results indicate that the floral fraction presents a significantly lower toxicological risk, supporting its application in intelligent films, especially when there is no direct contact with food.

Thus, although several plant sources are widely used in the production of pH-sensitive films, the use of anthocyanins extracted from *Catharanthus roseus* presents potential advantages. This ornamental species is easily cultivated, widely distributed, and flowers throughout the year, ensuring a continuous and sustainable source of anthocyanins, without competing with food resources. In addition, the extracts of *C. roseus* demonstrated adequate sensitivity to pH variations, with distinct and stable chromatic changes, comparable to those observed in other traditional sources. These attributes indicate that *C. roseus* may be a viable and promising alternative for the development of intelligent films, expanding the possibilities of sustainable formulations for colorimetric freshness indicators.

3.3. Characterization of the physical, structural and morphological properties of the films

The thickness values of the films incorporated with anthocyanin extracts ranged from 0.116 to 0.102 mm (Table 3), with a tendency to decrease proportionally to the increase in the concentration of the extract. This behavior can be attributed to two main mechanisms: i) dilution of the polymeric matrix caused by the incorporation of the anthocyanin extract, resulting in lower viscosity of the filmogenic solution, and ii) specific interactions between anthocyanins and the structural components of the film (collagen, pectin, and glycerol), promoting a more compacted rearrangement of the polymeric chains. These results are similar to those reported for films with dye extract from petunia flowers on a colorimetric sensor [70].

The analysis of the optical properties (Table 3) showed that the incorporation of the extract caused a significant reduction in both the transparency and luminosity (L*) of the films, especially at the concentration of 30 %. These changes in optical properties can be attributed to the scattering and absorption of visible light by the anthocyanins present in the extract. Higher opacity can help prevent color fading and anthocyanin instability, especially with exposure to UV radiation [71]. Similar behavior was observed by Qiu et al. [72] in sodium alginate/apricot peel pectin films incorporated with anthocyanins from roses.

The addition of CAE gave the films a wine coloration, intensified proportionally to the concentration of the extract (Fig. 3A). This color change was evidenced by the increase in the values of a* and b*. The total colorimetric variation (ΔE) showed a direct correlation with the concentration of CAE in the films, reaching a maximum value at the highest concentration tested.

Color analysis of the films after 40 days of storage at 25 °C indicated an increase in a* and b* values (Table 3), suggesting a transition to redder and yellower hues. These changes may be attributed to the degradation of anthocyanins present in the extract, evidenced by the reduction in the total anthocyanin content of the CAE, or to chemical reactions with the polymer matrix. Similar results were reported by Romruen et al. [73], who observed chromatic variations in intelligent

Table 3
Thickness, mechanical properties, solubility, WPV, transparency, color and degradability of films.

Parameters		C	F10	F20	F30	*P*-value
Thickness (mm)		0.116 ± 0.005^{a}	0.106 ± 0.005^{ab}	0.104 ± 0.005^{b}	0.102 ± 0.008^{b}	0.0139
TS (MPa)		5.294 ± 0.651^{a}	5.059 ± 0.822^{a}	4.686 ± 0.011^{a}	4.542 ± 1.386^{a}	0.8168
Elongation at break (%)		20.842 ± 1.051^{a}	19.185 ± 0.795^{ab}	19.131 ± 0.659^{ab}	16.981 ± 1.202^{b}	0.0653
WVP (10^{-8} g /m s Pa)		5.41 ± 0.262^{a}	6.02 ± 0.820^{a}	6.65 ± 0.453^{a}	6.65 ± 0.396^{a}	0.1909
Water solubility (%)		100 ± 0.000^{a}	100 ± 0.000^{a}	100 ± 0.000^{a}	100 ± 0.000^{a}	<0.001
Transparency (%)		2.853 ± 0.000^{ab}	2.858 ± 0.001^{a}	2.843 ± 0.000^{b}	2.824 ± 0.003^{c}	<0.001
Color	L*	84.95 ± 0.042^{a}	83.43 ± 0.184^{b}	78.3 ± 0.523^{c}	74.45 ± 0.155^{d}	<0.001
	a*	−0.47 ± 0.014^{c}	1.06 ± 0.028^{c}	2.375 ± 0.190^{b}	4.535 ± 0.459^{a}	<0.001
	b*	7.695 ± 0.190^{d}	9.11 ± 0.254^{c}	15.63 ± 0.480^{b}	20.96 ± 0.381^{a}	<0.001
ΔE			2.441 ± 0.141^{b}	16.084 ± 0.363^{b}	99.489 ± 0.660^{a}	<0.001
Weight loss by degradability test (%)	Day 7	1.771 ± 0.011^{b}	2.550 ± 0.291^{a}	1.175 ± 0.203^{bc}	0.883 ± 0.030^{c}	0.0025
	Day 15	3.265 ± 0.010^{a}	3.677 ± 0.011^{a}	2.126 ± 0.055^{b}	1.216 ± 0.212^{c}	<0.001
	Day 30	5.670 ± 0.162^{a}	4.189 ± 0,051^{b}	3.564 ± 0.180^{b}	2.564 ± 0.417^{c}	<0.001
	Day 60	33.231 ± 0.733^{a}	31.399 ± 0.474^{b}	32.007 ± 0.057^{ab}	29.888 ± 0.127^{c}	0.0073
Color film (40 day)	L*	93.41 ± 0.395^{a}	83.25 ± 0.042^{b}	76.905 ± 0.007^{c}	69.30 ± 0.593^{d}	<0.001
	a*	−0.59 ± 0.282^{a}	2.025 ± 0.007^{b}	5.695 ± 0.009^{c}	10.905 ± 0.629^{d}	<0.001
	b*	9.450 ± 0.537^{d}	29.40 ± 0.212^{c}	36.205 ± 0.883^{b}	39.715 ± 0.827^{a}	<0.001
Color film 40 days (exposed storage with 10 % ammonia)	L*	91.07 ± 0.538^{a}	83.55 ± 0.184^{b}	74.300 ± 0.693^{c}	73.465 ± 0.148^{c}	<0.001
	a*	−1.05 ± 0.045^{a}	−0.4 ± 0.214^{b}	4.25 ± 0.385^{c}	4.745 ± 0.134^{c}	<0.001
	b*	9.770 ± 1.417^{a}	31.65 ± 1.357^{b}	40.61 ± 2.729^{c}	44.07 ± 2.602^{c}	<0.001
ΔE		2.41 ± 0.121^{a}	3.32 ± 0.071^{b}	5.32 ± 0.145^{c}	8.82 ± 0.250^{d}	<0.001

FC: control; F10: 10 of CAE; F8: 20 of CAE; F30: 30 of CAE. WVP: Water Permeability Vapor. TS: Tensile Strength. Values are mean ± standard deviation. Each value consists of 3 independent measurements, except thickness ($n = 10$), elongation at break ($n = 6$) and color ($n = 12$). The means followed by the same letter do not differ statistically from each other by the Tukey test at the 5 % probability level ($p < 0.05$).

films containing natural pigments, and by Taylor and Francis [74], who associated these changes with dye instability during storage.

Regarding the mechanical properties of the films (Table 3), no variation was observed in the tensile strength (TS), which presented values between 4.542 MPa and 5.294 MPa. Similar results were found by Liu et al. [75] on polylactide-based intelligent films embedded with butterfly pea flower extract (4.40 MPa and 7.50 MPa). In contrast, the addition of anthocyanins from red cabbage was associated with a decrease in the tensile strength of cellulose-based films [76]. However, the present study was able to incorporate higher concentrations of anthocyanin-rich CAE without substantially compromising the strength of the films. The elasticity of the films, however, showed a significant reduction with the increase in CAE concentration. High levels of anthocyanins can weaken the interactions between the macromolecules of the film's polymeric matrix, compromising the membrane structure and impairing its mechanical properties [77]. Similar results were observed by Zhang et al. [71] in indicator films based on κ-carrageenan, butterfly pea flower anthocyanin, and nano titanium dioxide. Despite this mechanical limitation, the films did not present limitations in their applicability and anthocyanins offer functional benefits such as improved antioxidant properties and pH sensitivity, justifying their incorporation into the developed films.

Regarding solubility, the results indicated that there was no significant variation between the treatments, with all formulations achieving 100 % solubilization in water. This characteristic can be explained by the hydrophilic nature of the film components (collagen, pectin, and anthocyanins), whose groups establish hydrogen bonds with water, a typical behavior of phenolic acids and flavonoids found in vegetables [78]. Similar results were reported by Gasti et al. [79] on chitosan/methylcellulose intelligent films with anthocyanin from *Phyllanthus reticulatus*. This high solubility in water directs the application of the material developed as a headspace film, where it can act as a barrier or indirect interaction with the product, without dissolution or direct interference with the characteristics of the food.

The water vapor permeability test did not show significant variation between treatments, with values between 5.4 and 6.7 × 10^{-8} g/m s Pa (Table 3). This behavior corroborates the results found by Kim et al. [80], who reported similar values (7.6 × 10^{-8} g/m s Pa) in films incorporated with butterfly pea anthocyanins. In contrast, Wu et al. [81] observed a significant reduction in the WVP of films after the addition of *Clitoria ternatea* L extract, attributing this effect to the specific interactions between anthocyanins and polymer matrix. Maintaining low WVP values is desirable to minimize gas exchange and preserve the quality of the packaged product.

The structural characterization of the films by FT-IR spectroscopy (Fig. 1A-B-C-D) revealed characteristic bands at 3527 cm^{-1} (pectin) and 3315 cm^{-1} (glycerol), associated with the stretching vibrations of the –OH groups, typical of polysaccharides and polyalcohol. The extract obtained showed a band at 3381 cm^{-1}, indicating the presence of hydroxyl groups. Peaks in a similar region were observed in the extract (1651 cm^{-1}) and pectin (1645 cm^{-1}), attributed to stretching vibrations of the C═O bonds, characteristics of an amide or carboxylic structures in phenolic compounds, and carboxylate groups in galacturonic acids, respectively. The glycerol showed an intense band at 1031 cm^{-1}, corresponding to the C—O stretching of ester or alcohol bonds present in the structures of the compounds analyzed [82].

In Fig. 1E, it was observed that the films containing CAE presented spectral patterns similar to those of the control film, indicating that the incorporation of the extract did not alter the chemical structure of the films. However, small variations in the intensity of the peaks were detected, with maintenance of the characteristic bands: stretching of the –OH groups, vibration of the C—H bonds (–CH_2), C═O stretching (amide-I) and C—O bonds. Similar behavior was reported by Jiang et al. [6] in longan seed starch films incorporated with anthocyanin extract from the bracts of banana flower. These results indicate that the addition of CAE did not cause significant chemical changes in the structures of the analyzed films, preserving the integrity of the spectral properties of the materials.

The evaluation of the biodegradability of the films revealed distinct degradation patterns over 60 days of exposure to the soil (Table 3). The results showed that during the first seven days, the F20 and control

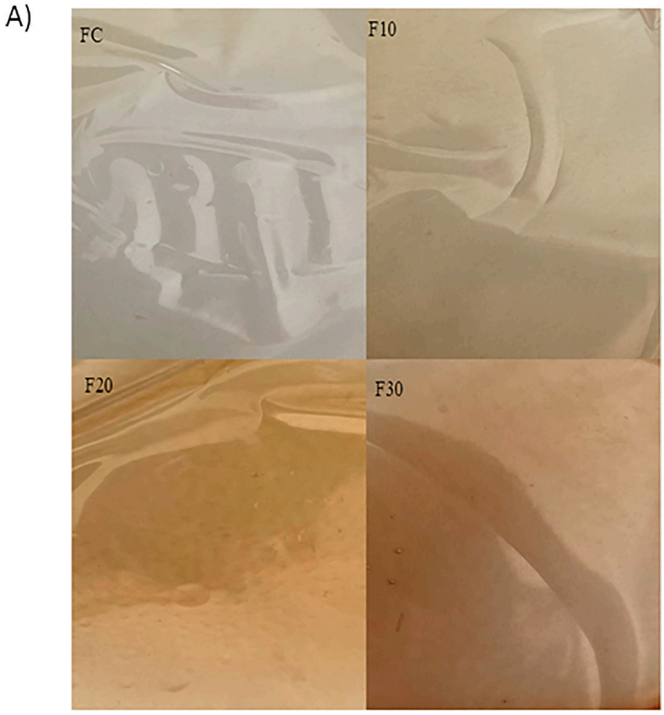

Fig. 3. Characterization of the physical, structural and morphological properties of the films A) Picture films; B) XDR curve; C) Micrography of the bioplastics surface and cross-section; D) TG curve; E) DSC curve; F) Antioxidant activity of films ABTS and FRAP. FC: control; F10: 10 of CAE; F8: 20 of CAE; F30: 30 of CAE. FC_T: control cross-sectional; $F10_T$: 10 of CAE cross-sectional; $F20_T$: 20 of CAE cross-sectional; $T30_T$: 30 of CAE cross-sectional. FC_S: control surface; $T10_S$: 10 of CAE surface; $T20_S$: 20 of CAE surface; $T30_S$: 30 of CAE surface.

treatments did not differ from each other, with F30 and F10 being the films with the lowest and highest percentage of degradation on this day, respectively. On the 15th day, the control treatment showed a degradation rate of 3.265 %, with no difference in F10, while F30 had the lowest rate (1.216 %). The greater degradation of the F10 film on days 7 and 15 may be associated with the lower concentration of phenolic compounds, which possibly acted as secondary plasticizers, increasing the mobility of the polymer matrix and favoring degradation in the initial phase. This effect was attenuated with treatments using higher concentrations of the extract, which provided greater structural stability to the films [83]. At 30 days of exposure, there was no significant difference in the degradation rate between F10 and F20, while F30 maintained the lowest degradation (2.564 %). After 60 days, the F30 treatment, with the highest concentration of anthocyanins, had the lowest degradation (33.231 %), suggesting that the presence of these bioactive compounds contributes to the reduction of the degradation rate of the films. This phenomenon can be attributed to the antioxidant properties of anthocyanins, which, in addition to giving color to the films, slow down oxidative degradation [84]. These findings corroborate previous studies on the incorporation of antioxidant compounds into biodegradable films [85,86].

The FT-IR analysis of the films after 60 days of exposure to soil (Fig. 1F) confirmed the structural changes resulting from the biodegradation process. Variations in the intensity of the peaks were observed, indicating changes in the chemical bonds of the materials over time. The characteristic peaks of the elongation vibration of the –OH groups, of the C—H bonds in the $–CH_2$ groups, of the C═O bonds in the amide-I groups, and of the C—O bonds, typical of the film components, showed greater intensity in the F30 treatment. This observation suggests that, although the degradation process occurred, the higher concentration of anthocyanins contributed to the maintenance of the stability of the molecular structure throughout the evaluated period.

The crystal structure of the films was analyzed by X-ray diffraction, as illustrated in Fig. 3B. The control film presented four total peaks, with three wide diffraction peaks, observed at 9.72°, 13.44° and 28.68° that were attributed to the amorphous structure. The sharp and well-defined peak at 21.90° indicated the presence of semicrystalline structures. When CAE was incorporated into the films, a reduction in the intensity of the characteristic peaks of the semicrystalline structures was observed, with a progressive decrease in crystallinity proportional to the increase in the concentration of the extract. The appearance of new peaks with amorphous characteristics suggests the formation of hydrogen bonds between the anthocyanins of the CAE and the polymer matrix, resulting in a decrease in the crystallinity of the samples. Similar behavior was observed by Amaregouda et al. [87] in intelligent films based on chitosan/polyvinyl alcohol matrices containing anthocyanin from *Jacaranda cuspidifolia.* The predominance of amorphous regions gives the films desirable technological properties, such as greater deformability, elasticity, and malleability [88].

The morphology of the surface and cross-section of the films was analyzed by scanning electron microscopy (SEM), as shown in Fig. 3C. Superficial micrographs showed an association between the increase in CAE concentration and the development of progressively smoother, more continuous and homogeneous surfaces, corroborating the results obtained by X-ray diffraction.

The mechanical behavior of the films in relation to tear strength seems to be associated with the morphological characteristics of the samples analyzed. To investigate this hypothesis, the cross-section analysis of the films used in the tensile analysis was performed. The control film showed fibrils aligned in the direction of the tear, indicating that the polymeric chains were oriented. This structural organization suggests greater fracture resistance, since regions with greater molecular alignment tend to have greater crystallinity. In contrast, films containing CAE presented circular voids distributed in several regions, making them more susceptible to tearing under lower loads, when compared to fibrillar regions where the rupture of polymeric chains is necessary [89].

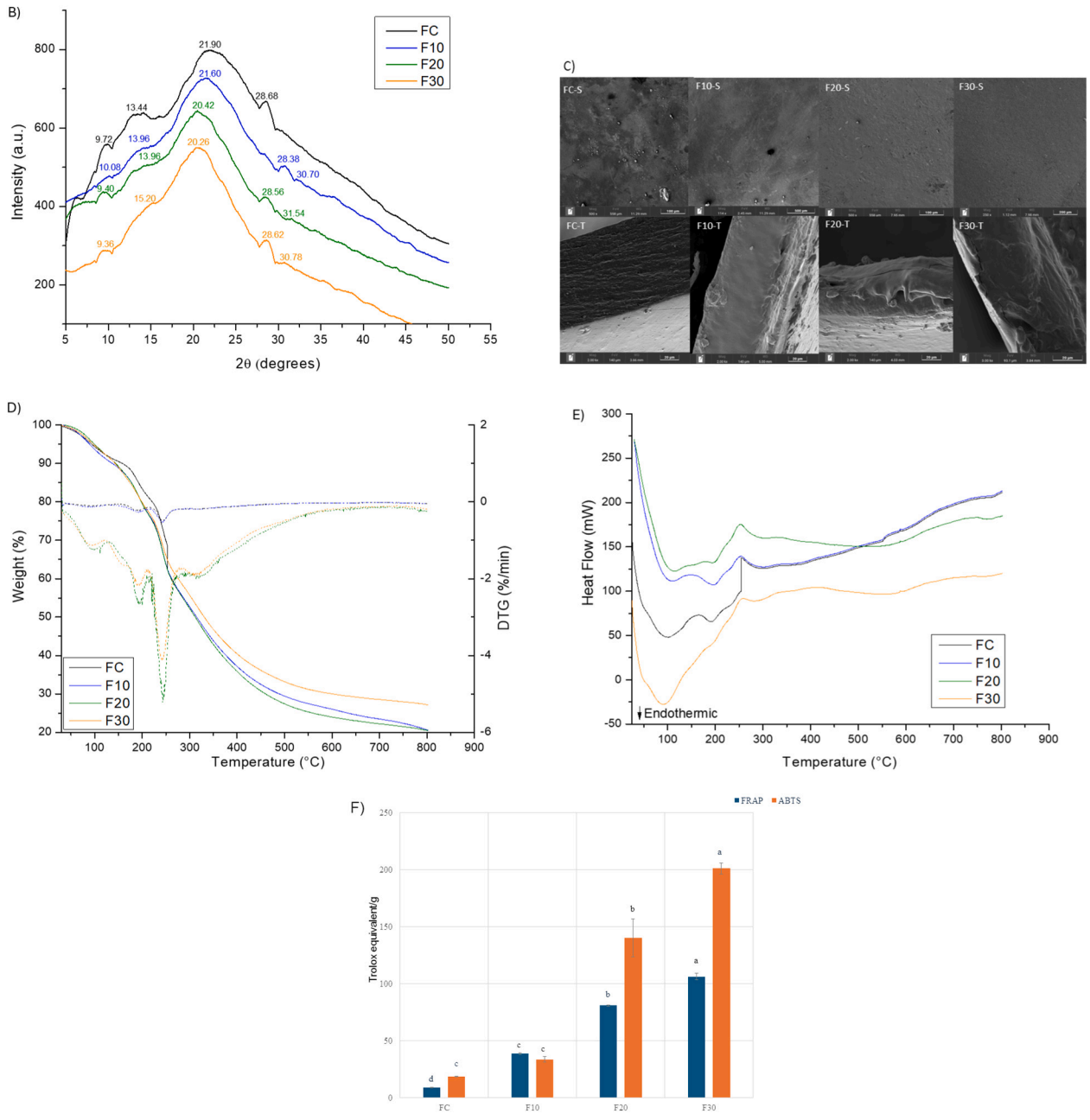

Fig. 3. (*continued*).

These morphological observations explain the reduction in elasticity and crystallinity of the films containing the extract.

The thermal properties of embedded films with different concentrations of CAE were evaluated by TGA and DSC. In the TGA analysis (Fig. 3D), four distinct stages of mass loss were identified. In general, the films showed higher thermal resistance compared to the control. The first stage, between 111 °C (control) and 120 °C (F10), was associated with the evaporation of surface water and residual solvents. The second stage, between 194 °C (control) and 219 °C (F10), corresponded to the release of intrinsic water from the film, with an increase in TG observed in the treated samples attributed to the hydrogen interactions between anthocyanins and the polymer matrix, according to the results of FT-IR. The third stage, between 250 °C (F20 and F30) and 260 °C (F10), was related to the decomposition of polysaccharides, protein chains and anthocyanins. The fourth stage, between 303 °C (control) and 334 °C (F20), represented the final decomposition of the residual matrix.

The F10 formulation showed higher thermal stability in most stages, possibly due to the presence of thermally stable structures, such as the aromatic rings of anthocyanins [90]. However, higher concentrations of CAE resulted in a slight reduction in thermal stability, a behavior like that found by Freitas et al. [91] in studies with rice straw extracts. The final residue after heating was approximately 21 % for the control film and F10, 20 % for F20 and 27 % for F30, indicating greater thermal mass loss at high concentrations of CAE (30 %). However, the films maintained thermal stability superior to the control.

DSC analysis (Fig. 3E) identified an endothermic peak characteristic of the melting process, with higher temperatures in films with up to 20 % CAE. The peak melting was shifted from 101 to 191 °C (control) to 112–196 °C (F20), suggesting the presence of crystalline substances with degradation at different temperatures [78]. The F30 formulation showed a lower melting temperature and absence of evident crystallinity peaks, corroborating the data of XRD, TGA and SEM regarding lower crystallinity and thermal stability at high concentrations of CAE. Santos et al. [45] showed that the addition of amber extract in PLA films

reduced the crystallization rate and melting temperature. Despite the thermal changes, the use of these films as intelligent packaging does not compromise their efficiency or applicability.

The antioxidant capacity of the films, evaluated by the FRAP and ABTS methods (Fig. 3F), showed an increase proportional to the concentration of CAE added, attributed to the presence of phenolic compounds in the *Catharanthus roseus* flower. Among the phenolic compounds with the highest antioxidant activity in both methods, quercetin, catechins, epicatechins, and resveratrol stand out, all identified in CAE [92]. The F30 films showed higher values (106.09 μmol Trolox/g for FRAP and 201.13 μmol Trolox/g for ABTS) compared to the control (8.8 μmol Trolox/g and 18.49 μmol Trolox/g, respectively). The higher antioxidant activity measured by the ABTS method, compared to FRAP, can be attributed to differences in evaluation mechanisms: while ABTS quantifies the ABTS cationic radical scavenging capacity, FRAP evaluates the reducing power of antioxidants [93]. This methodological difference can lead to variations in the release and efficacy of the active compounds present in the extracts. The potentiating effect of anthocyanins on the antioxidant properties of biopolymeric films has been widely documented in the literature [6,9,11,94].

3.4. Characterization of the functional properties of the films

The validation of the intelligent film developed as an indicator of fish freshness was carried out through the evaluation of instrumental color parameters against nitrogenous volatile compounds (TVB-N), whose presence is directly associated with fish deterioration [95]. To simulate the degradation conditions, ammonia was used as a model compound, given its preponderant role among TVB-N compounds [96]. Fig. 4 illustrates the color variation (ΔE) of the films as a function of the different concentrations of ammonia in aqueous solution.

The interaction of the films with the ammonia solutions resulted in a change to yellowish hue (Fig. 8), with ΔE proportional to the concentration of CAE incorporated into the films. The color changes were noticeable to the naked eye, exceeding the threshold of human visual perception established at ΔE equal to or greater than 2 and quickly detected in less than 5 min [97]. The ΔE values gradually increased from 3.523 to 11.882 with the different treatments, even at the lowest ammonia concentration evaluated. The maximum variation was observed in the F30 treatment with 10 % ammonia. At concentrations higher than 20 % of ammonia, the colorimetric changes reached a plateau, remaining constant in all treatments.

After 40 days of storage, the films still showed a significant color response when exposed to 10 % ammonia (Table 3). Although ΔE values

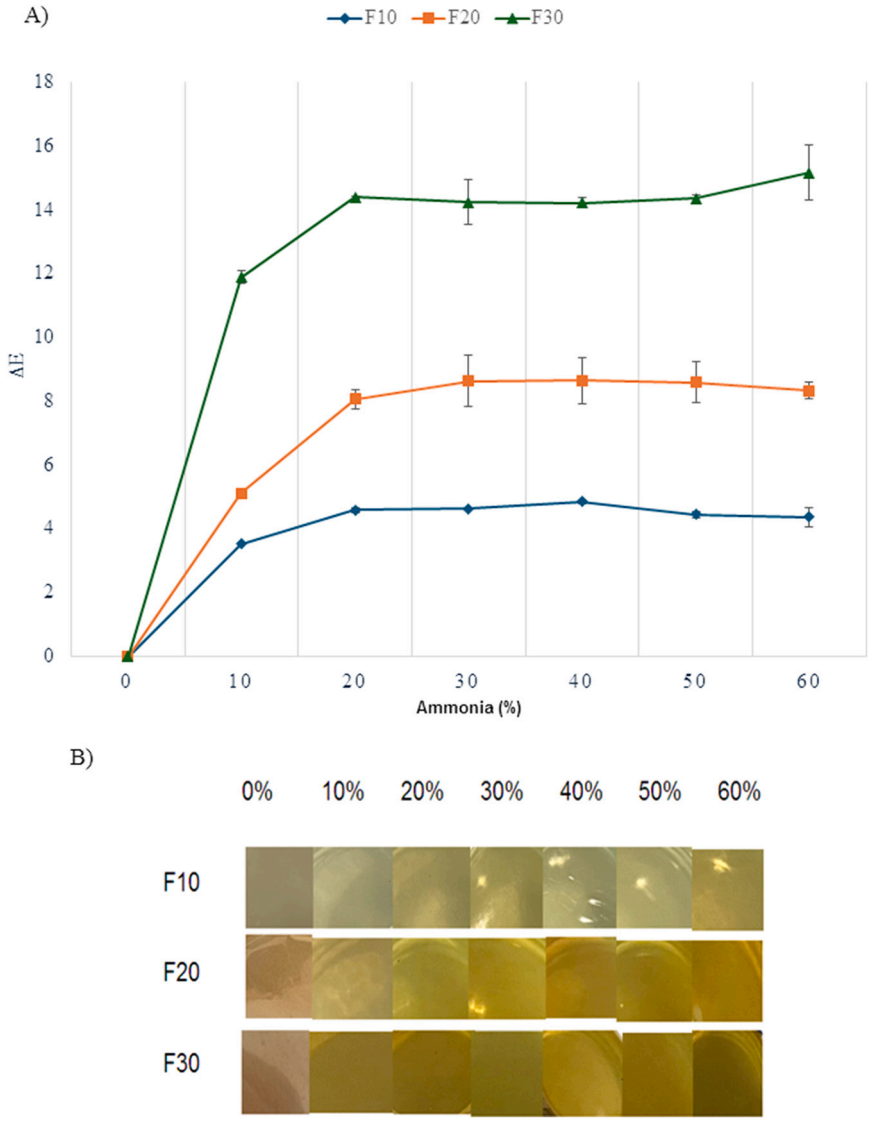

Fig. 4. The color sensitivity A) and changes (B) to different ammonia concentrations of films. F10: 10 of CAE; F20: 20 of CAE; F30: 30 of CAE.

were lower than those observed in freshly produced films, the color variation remained noticeable, especially in formulations with higher extract concentrations, reaching ΔE of up to 8.82. These results indicate that, even after prolonged storage, the films maintain their visual responsiveness to volatile alkaline compounds, reinforcing their potential as intelligent indicators for monitoring food spoilage.

The mechanism responsible for the color change is based on the volatilization of ammonia and its subsequent interaction with the films. The nucleophilic nature of ammonia promotes the deprotonation of anthocyanins, altering the charge distribution of these molecules. This structural modification results in changes in the wavelength of absorbed photons, manifesting as a change in the perceived coloration of the films [98,99]. Consequently, films with higher anthocyanin concentrations showed more pronounced color changes due to the greater availability of sites for deprotonation.

3.5. Application of the films in the detection of freshness of tilapia fish

The potential of collagen films with anthocyanins from *Catharanthus roseus* as indicators of freshness and food spoilage was evaluated, using tilapia fillet as a model. This choice was based on the deterioration process characteristic of fish, in which the action of microorganisms and enzymes on proteins results in the formation of volatile nitrogenous substances, causing an increase in the pH of the environment [100]. The fillets were stored at room temperature to accelerate the deterioration process, allowing the evaluation of the response of the intelligent films. The choice of this condition was based on similar approaches described by Fallah et al. [101], Oduse et al. [102], and Shi et al. [103].

In the performed experiments (Fig. 5A, B and C), the pH of the fish stored at room temperature exceeded 6.5 after 24 h, signaling the beginning of deterioration. This increase is associated with the onset of autolytic deterioration, in which muscle proteins are degraded by endogenous proteases and alkaline microorganisms, resulting in the formation of volatile compounds, such as ammonia, dimethylamine, and trimethylamine, and consequently, an increase in pH [104]. The color change in the packaging was observed, especially in the F30 treatment, which went from translucent to a yellow tone with a tendency to opaque green. In the F20 treatment, the color change was visible only when the pH exceeded 7, while in the F10 treatment there was no noticeable change in color, despite the deterioration of the fish. Said and Sarbon [105] observed an increase in pH from 6.26 to 7.76 in four days of storage, when monitoring the freshness of fish fillets using gelatin films incorporated with curcumin extract.

Graphical analysis of the data revealed a positive linear correlation

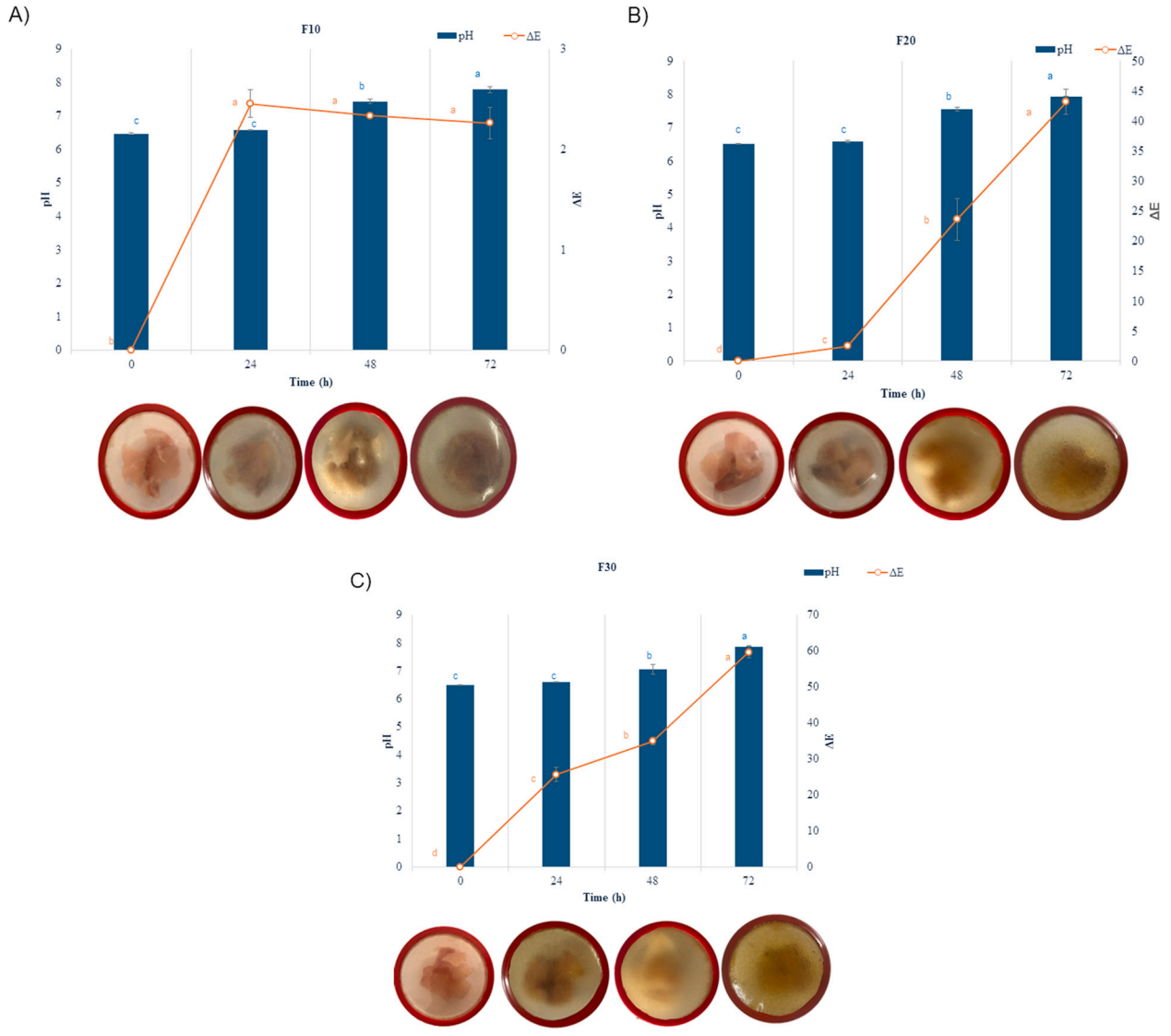

Fig. 5. Application of indicator packaging and linear model between ΔE of the film and pH of the fish during storage time: A) F10, B) F20 and C) F30, evaluated by headspace in tilapia fillet. FC: control; F10: 10 of CAE; F20: 20 of CAE; F30: 30 of CAE.

between ΔE and pH increase in F20 and F30 treatments, corroborating previous studies that highlight the use of natural pigments in biopolymer films as an effective tool to monitor food safety and quality [6,106]. The results indicate that the film with 30 % *Catharanthus roseus* extract can detect deterioration at an early stage and can serve as an efficient monitor of fish freshness, such as tilapia, in real time.

4. Conclusion

In this study, we investigated the potential of *Catharanthus roseus* flower extract and its impact on the properties of collagen-based films. The extract has a high concentration of anthocyanins, phenolic compounds, and antioxidant activity, with the ability to change its color in response to pH variations. The incorporation of the extract into bioplastics improves resistance to degradation, resulting in a more homogeneous and smaller crystalline microstructure, with light barrier properties, suggesting its potential in food protection. Although high concentrations of anthocyanins negatively impacted the elasticity and thermal stability of the films, these effects did not compromise their practical application, allowing safe handling and use in packaging without the risk of breakage or premature degradation.

The development of the intelligent packaging system demonstrated technical feasibility in indicating the fish deterioration process, using tilapia fillets as a model. F30 detected fish deterioration at an early stage, offering a non-invasive and environmentally responsible approach to quality monitoring. The application of these films represents a technological innovation with the potential to improve quality control and traceability in the fishing industry.

The use of collagen extracted from waste from the fishing industry as a polymeric matrix for biodegradable films represents an approach aligned with the principles of the circular economy, contributing to the reduction of environmental impacts associated with conventional plastic materials. Future studies may focus on developing effective stabilization strategies for anthocyanin extracts, such as encapsulation, and on assessing the long-term stability of the films under different environmental conditions and storage periods, thereby enhancing their industrial application.

CRediT authorship contribution statement

Gabrielle Ingrid Bizerra Florentino: Writing – review & editing, Writing – original draft, Investigation, Formal analysis, Data curation. **Cristiani Viegas Brandão Grisi:** Writing – review & editing, Writing – original draft, Validation, Supervision, Investigation, Funding acquisition, Data curation, Conceptualization. **Marcos dos Santos Lima:** Writing – original draft, Methodology, Funding acquisition, Formal analysis. **Rita de Cassia Andrade da Silva:** Writing – original draft, Methodology, Formal analysis. **Valquíria Cardoso da Silva Ferreira:** Writing – original draft, Methodology, Formal analysis, Data curation. **Ângela Maria Tribuzy de Magalhães Cordeiro:** Writing – original draft, Validation, Resources, Methodology, Investigation, Funding acquisition. **Fábio Anderson Pereira da Silva:** Writing – review & editing, Validation, Resources, Project administration, Methodology, Funding acquisition, Data curation, Conceptualization.

Declaration of competing interest

The authors declare that they have no known competing financial interests or personal relationships that could have appeared to influence the work reported in this paper.

Acknowledgements

The authors acknowledge the Coordination for the Improvement of Higher Education Personnel (CAPES) for financial support and scholarships to the first author (G. I. B. Florentino). They also thank the National Council for Scientific and Technological Development (CNPq) for the financial support through the project 313663/2021-1. The authors acknowledge the laboratories NPE-LACOM, LAQA, LAMAB, LAPAMA and LABFILM, belonging to the Federal University of Paraiba (UFPB), and the laboratory LBCL belonging to the Federal Institute of Sertão Pernambucano (IFSertao-PE) for providing the essential infrastructure and support for the development of this work.

Data availability

Availability of data and materials data are available by contacting the authors.

References

[1] S. Liaqat, M. Hussain, J. Riaz, Entry of microplastics into the food chain and the food supply chain, Microplastic Pollut. (2024) 289–306, https://doi.org/10.1007/978-981-99-8357-5_17.
[2] B. Saiprasad, G.S. Sagar, K.S. Ashish, S. Bhautik, K. Tejaswini, R.D. Gautam, Microplastic (MP) pollution in aquatic ecosystems and environmental impact on aquatic animals, Uttar Pradesh J. Zool. 45 (2024) 59–68, https://doi.org/10.56557/upjoz/2024/v45i53931.
[3] S.G. Ricardo, T.G.A. Esmeralda, D.I. Alejandro, O.V. Gabriel, Use of the aquatic lily (Eichhornia crassipes) as an alternative in the generation of bioplastics, Cienc. Lat. Multidiscip. Sci. J. 8 (2024) 9621–9637, https://doi.org/10.56557/upjoz/2024/v45i53931.
[4] E.M.P.X. Neves, R.R. Pereira, G.V. da Silva Pereira, L.L. Vieira, L.D.F.H. Lourenço, Effect of polymer blend on the development of bioplastics from fish waste, Bull. Fish. Inst. 45 (2019) 1–10, https://doi.org/10.20950/1678-2305.2019.45.4.518.
[5] S. Vijayakumar, J. Chen, Z.I. González-Sánchez, K. Tungare, M. Bhori, H. Shakila, P. Anbu, Biomedical and ecosafety assessment of marine fish collagen capped silver nanoparticles, Int. J. Biol. Macromol. 260 (2024) 129324, https://doi.org/10.1016/j.ijbiomac.2024.129324.
[6] H. Jiang, W. Zhang, J. Cao, W. Jiang, Development of biodegradable active films based on longan seed starch incorporated with anthocyanin extracts from banana flower bracts and applications in food freshness indication, Int. J. Biol. Macromol. 251 (2023) 126372, https://doi.org/10.1016/j.ijbiomac.2023.126372.
[7] World Health Organization (WHO), Food Safety, WHO, 2024. https://www.who.int/news-room/fact-sheets/detail/food-safety (accessed 01 March 2025).
[8] K. Ganeson, G.K. Mouriya, K. Bhubalan, M.R. Razifah, R. Jasmine, S. Sowmiya, S. Ramakrishna, Smart packaging– a pragmatic solution to approach sustainable food waste management, Food Packag. Shelf Life 36 (2023) 101044, https://doi.org/10.1016/j.fpsl.2023.101044.
[9] R. Li, S. Wang, H. Feng, D. Zhuang, J. Zhu, A chitosan/gelatin smart film via improving the accuracy of anthocyanin-induced color recognition for monitoring under-freshness differentiation of beef 146 (2024) 109219, https://doi.org/10.1016/j.foodhyd.2023.109219.
[10] L. Liu, W. Wu, L. Zheng, J. Yu, P. Sun, P. Shao, Intelligent packaging films incorporated with anthocyanins-loaded ovalbumin-carboxymethyl cellulose nanocomplexes for food freshness monitoring, Food Chem. 387 (2022) 132908, https://doi.org/10.1016/j.foodchem.2022.132908.
[11] L. Wang, C. Yang, X. Deng, J. Peng, J. Zhou, G. Xia, H. Yang, A pH-sensitive intelligent packaging film harnessing *Dioscorea zingiberensis* starch and anthocyanin for meat freshness monitoring, Int. J. Biol. Macromol. 245 (2023) 125485, https://doi.org/10.1016/j.ijbiomac.2023.125485.
[12] M. Ranjbar, M.H.A. Tabrizzad, G. Asadi, H. Ahari, Investigating the microbial properties of sodium alginate/chitosan edible film containing red beetroot anthocyanin extract for smart packaging of chicken fillet as a pH indicator, Heliyon 9 (2023) e18879, https://doi.org/10.1016/j.heliyon.2023.e18879.
[13] F. Yi, F. Hou, S. Zhan, L. Song, R. Zhang, X. Han, Z. Liu, Preparation, characterization and application of pH-responsive smart film based on chitosan/zein and red radish anthocyanin, Int. J. Biol. Macromol. 253 (2023) 127037, https://doi.org/10.1016/j.ijbiomac.2023.127037.
[14] Y.A. Chim-Chi, A.R. Fernández-Méndez, E. Pérez-Pacheco, J.C. Canto-Pinto, R. J. Estrada-León, A. Ortiz-Fernández, Y. Pérez-Padilla, Development of pH indicator smart packaging films with anthocyanins from the purple star apple shell (*Chrysophyllum cainito* L.), J. Food Meas. Charact. 18 (2024) 2651–2660, https://doi.org/10.1007/s11694-023-02344-2.
[15] F. Zeng, Y. Ye, J. Liu, P. Fei, Intelligent pH indicator composite film based on pectin/chitosan incorporated with black rice anthocyanins for meat freshness monitoring, Food Chem.: X 17 (2023) 100531, https://doi.org/10.1016/j.fochx.2022.100531.
[16] W. Wu, L. Zheng, J. Yu, L. Liu, G. Goksen, P. Shao, High-sensitivity intelligent packaging films harnessing rose anthocyanins and hydrophilic silica aerogel for visual food freshness monitoring, Food Qual. Saf. 8 (2024) fyad051, https://doi.org/10.1093/fqsafe/fyad051.
[17] A.F.D. Santos, L.T.D. Santos, M.P.D. Nascimento, E.L.D. Oliveira, T.G. Ribeiro, F. D. Pereira, G.G. Pereira, Review of three medicinal and ornamental species of the family Apocynaceae Juss, Res. Soc. Dev. 11 (2022) e1011224876, https://doi.org/10.33448/rsd-v11i2.24876.

[18] A.J. Afolayan, T.O. Sunmonu, In vivo studies on antidiabetic plants used in South African herbal medicine, J. Clin. Biochem. Nutr. 47 (2010) 98–106, https://doi.org/10.3164/jcbn.09-126R.
[19] G.F. Costa, C.V.B. Grisi, B.R.L.A. Meireles, S. Sousa, A.M.T.M. Cordeiro, Collagen films, cassava starch, and their blends: physical–chemical, thermal and microstructure properties, Packag. Technol. Sci. 35 (3) (2022) 229–240, https://doi.org/10.1002/pts.2621.
[20] AOAC, Hydroxyproline in meat and meat products (Method 990.26), in: Off. Methods Anal, 17th ed, 2000. Gaithersburg, MD.
[21] V. Villani, G. Di Marco, F. Iacovelli, D. Pietrucci, A. Canini, A. Gismondi, Profile and potential bioactivity of the miRNome and metabolome expressed in *Malva sylvestris* L. leaf and flower, BMC Plant Biol. 23 (1) (2023) 439.
[22] CIE, Colorimetry: Understanding the System CIE, Colorimetria, 2007, pp. 25–78.
[23] E.J. Jeyaraj, Y.Y. Lim, W.S. Choo, Antioxidant, cytotoxic, and antibacterial activities of *Clitoria ternatea* flower extracts and anthocyanin-rich fraction, Sci. Rep. 12 (1) (2022) 14890, https://doi.org/10.1038/s41598-022-19146-z.
[24] R. Re, N. Pellegrini, A. Proteggente, A. Pannala, M. Yang, C. Rice-Evans, Antioxidant activity applying an improved ABTS radical cation decolorization assay, Free Radic. Biol. Med. 26 (9–10) (1999) 1231–1237, https://doi.org/10.1016/S0891-5849(98)00315-3.
[25] I.F.F. Benzie, J.J. Strain, Ferric reducing capacity of plasma (FRAP) as a measure of "antioxidant power: the FRAP assay", Anal. Biochem. 239 (1996) 70–76, https://doi.org/10.1006/abio.1996.0292.
[26] L.M. dos Santos, B.S. Dantas, A.J.D.B.A. Carvalho, G.E. Pereira, T.C. Pimentel, M. Magnani, A novel method for ultra-fast determination of phenolics with performance comparable to UPLC/DAD: method development and validation on analysis of seedless table grapes, J. Food Compos. Anal. 134 (2024) 106511, https://doi.org/10.1016/j.jfca.2024.106511.
[27] ASTM, ASTM D882-12 Standard Test Method for Tensile Properties of Thin Plastic Sheeting, Am. Soc. Test. Mater, 2012.
[28] S.M. Ojagh, M. Rezaei, S.H. Razavi, S.M.H. Hosseini, Effect of chitosan coatings enriched with cinnamon oil on the quality of refrigerated rainbow trout, Food Chem. 120 (1) (2010) 193–198, https://doi.org/10.1016/j.foodchem.2009.10.006.
[29] ASTM, ASTM E96/E96M-16 Standard Test Methods for Water Vapor Transmission of Materials, Am. Soc. Test. Mater, 2016.
[30] R. Chandra, R. Rustgi, Biodegradation of maleated linear low-density polyethylene and starch blends, Polym. Degrad. Stab. 56 (2) (1997) 185–202, https://doi.org/10.1016/S0141-3910(96)00212-1.
[31] C. Spagnol, E.H. Fragal, A.G. Pereira, C.V. Nakamura, E.C. Muniz, H.D. Follmann, A.F. Rubira, Cellulose nanowhiskers decorated with silver nanoparticles as an additive to antibacterial polymers membranes fabricated by electrospinning, J. Colloid Interface Sci. 531 (2018) 705–715, https://doi.org/10.1016/j.jcis.2018.07.096.
[32] L.X. Mei, A.M. Nafchi, F. Ghasemipour, A.M. Easa, S. Jafarzadeh, A.A. Al-Hassan, Characterization of pH sensitive sago starch films enriched with anthocyanin-rich torch ginger extract, Int. J. Biol. Macromol. 164 (2020) 4603–4612, https://doi.org/10.1016/j.ijbiomac.2020.09.082.
[33] C. Bi, X. Li, Q. Xin, W. Han, C. Shi, R. Guo, J. Zhong, Effect of extraction methods on the preparation of electrospun/electrosprayed microstructures of tilapia skin collagen, J. Biosci. Bioeng. 128 (2019) 234–240, https://doi.org/10.1016/j.jbiosc.2019.02.004.
[34] H.A.G. Abdelaal, H.M.A. Mohamed, S.A. Saleh, R. Koriem, Characteristics and functional properties of collagen extracted from Nile tilapia (*Oreochromis niloticus*) skin, J. Mod. Res. 3 (2021) 36–43, https://doi.org/10.21608/JMR.2020.37541.1034.
[35] Z. Song, H. Liu, L. Chen, L. Chen, C. Zhou, P. Hong, C. Deng, Characterization and comparison of collagen extracted from the skin of the Nile tilapia by fermentation and chemical pretreatment, Food Chem. 340 (2021) 128139, https://doi.org/10.1016/j.foodchem.2020.128139.
[36] M.D.L.L.R. Menezes, H.L. Ribeiro, M.F. de Oliveira, J.P. Feitosa, Optimization of the collagen extraction from Nile tilapia skin (*Oreochromis niloticus*) and its hydrogel with hyaluronic acid, Colloids Surf. B: Biointerfaces 189 (2020) 110852, https://doi.org/10.1016/j.colsurfb.2020.110852.
[37] W.A. Lopes, M. Fascio, Scheme for interpretation of spectra of organic substances in the infrared region, Quím. Nova 27 (2004) 670–673, https://doi.org/10.1590/S0100-40422004000400025.
[38] Z.I. Elbialy, A. Atiba, A. Abdelnaby, I.I. Al-Hawary, A. Elsheshtawy, H.A. El-Serehy, D.H. Assar, Collagen extract obtained from Nile tilapia (*Oreochromis niloticus*) skin accelerates wound healing in a rat model by upregulating VEGF, bFGF, and α-SMA gene expression, BMC Vet. Res. 16 (2020) 1–11, https://doi.org/10.1186/s12917-020-02566-2.
[39] N. Reátegui-Pinedo, D. Salirrosas, L. Sánchez-Tuesta, C. Quiñones, S.R. Jáuregui-Rosas, G. Barraza, Z.A. Prieto, Characterization of collagen from three genetic lines (gray, red, and F1) from the skin of *Oreochromis niloticus* (tilapia) in young and old adults, Molecules 27 (2022) 1123, https://doi.org/10.1186/s12917-020-02566-2.
[40] T.R. Stella, C.M. Paraíso, J. dos Santos Pizzo, J.V. Visentainer, S.S. Dos Santos, G. S. Madrona, *Hibiscus sabdariffa* L. extracts freeze-dried and encapsulated by ionic gelation: an approach for yogurt application, J. Food Meas. Charact. 17 (2023) 2630–2638, https://doi.org/10.1007/s11694-023-01818-7.
[41] S. Lin, X. Meng, C. Tan, Y. Tong, M. Wan, M. Wang, Y. Ma, Composition and antioxidant activity of anthocyanins from *Aronia melanocarpa* extracted using an ultrasonic-microwave-assisted natural deep eutectic solvent extraction method, Ultrason. Sonochem. 89 (2022) 106102, https://doi.org/10.1016/j.ultsonch.2022.106102.
[42] G.C.V. Gamage, W.S. Choo, Hot water extraction, ultrasound, microwave and pectinase-assisted extraction of anthocyanins from blue pea flower, Food Chem. Adv. 2 (2023) 100209, https://doi.org/10.1016/j.focha.2023.100209.
[43] T.T.T. Nguyen, H.D. Nguyen, L.T. Tran, et al., Characterization of *Delonix regia* flowers' pigment and biological activities, Molecules 28 (7) (2023) 3243, https://doi.org/10.3390/molecules28073243.
[44] U.H. Zaidan, N.S. Kamaruzaman, F. Azhari, S.S.A. Gani, Anthocyanin stability and antioxidant capacity of *Clitoria ternatea* flower extract, Food Res. 8 (Suppl. 7) (2024) 59–66, https://doi.org/10.26656/fr.2017.8(S7).8.
[45] L.G. Santos, V.G. Martins, Optimization of the green extraction of polyphenols from the edible flower *Clitoria ternatea* by high-power ultrasound: a comparative study with conventional extraction techniques, J. Appl. Res. Med. Aromat. Plants 34 (2023) 100458, https://doi.org/10.1016/j.jarmap.2023.100458.
[46] A. Baştürk, B. Yavaş, Improving sunflower oil stability with propolis: a study on antioxidative effects of Turkish propolis during accelerated oxidation, J. Food Sci. 89 (2024) 8910–8929, https://doi.org/10.1111/1750-3841.17482.
[47] W. Bors, W. Heller, C. Michel, M. Saran, Flavonoids as antioxidants: determination of radical-scavenging efficiencies, Methods Enzymol. 186 (1990) 343–355, https://doi.org/10.1016/0076-6879(90)86128-i.
[48] Y.B. Kang, E.M. Koh, Improved stability of anthocyanins in aronia upon addition of chlorogenic acid, Korean J. Food Sci. Technol. 55 (6) (2023) 546–552, https://doi.org/10.9721/KJFST.2023.55.6.546.
[49] J. Wilska-Jeszka, A. Korzuchowska, Anthocyanins and chlorogenic acid copigmentation—influence on the colour of strawberry and chokeberry juices, Z. Lebensm. Unters. Forsch. 203 (1996) 38–42, https://doi.org/10.1007/BF01267767.
[50] R.S. Pal, Y. Pal, S. Punniyakotti, D. Katiyar, P. Kumari, Hesperidin: diversified prospects of naturally occurring bioflavonoid, Nat. Prod. J. 14 (3) (2024) 14–20, https://doi.org/10.2174/2210315514666230816141802.
[51] A. Escobar-Ortiz, E. Castaño-Tostado, N.E. Rocha-Guzmán, J.A. Gallegos-Infante, R. Reynoso-Camacho, Anthocyanins extraction from *Hibiscus sabdariffa* and identification of phenolic compounds associated with their stability, J. Sci. Food Agric. 101 (1) (2021) 110–119, https://doi.org/10.1002/jsfa.10620.
[52] V. Bhatt, N. Sendri, K. Swati, S.B. Devidas, P. Bhandari, Identification and quantification of anthocyanins, flavonoids, and phenolic acids in flowers of *Rhododendron arboreum* and evaluation of their antioxidant potential, J. Sep. Sci. 45 (14) (2022) 2555–2565, https://doi.org/10.1002/jssc.202200145.
[53] C. Colica, M. Milanović, N. Milić, V. Aiello, A. De Lorenzo, L. Abenavoli, A systematic review on natural antioxidant properties of resveratrol, Nat. Prod. Commun. 13 (9) (2018), https://doi.org/10.1177/1934578X1801300923.
[54] H. Luo, S. Deng, W. Fu, X. Zhang, X. Zhang, Z. Zhang, X. Pang, Characterization of active anthocyanin degradation in the petals of *Rosa chinensis* and *Brunfelsia calycina* reveals the effect of gallated catechins on pigment maintenance, Int. J. Mol. Sci. 18 (4) (2017) 699, https://doi.org/10.3390/ijms18040699.
[55] Q. Chen, X. Zhang, H. Yu, W. Yan, H. Tang, Changes of total anthocyanins and proanthocyanidins in the developing blackberry fruits, Int. J. ChemTech Res. 4 (1) (2012) 129–137.
[56] H. Liu, Z. Cheng, M. Luo, J. Xie, The dynamic variations of flavonoid metabolites in flower buds for *Zingiber miogaat* different developmental stages, J. Food Compos. Anal. 123 (2023) 105537, https://doi.org/10.1016/j.jfca.2023.105537.
[57] Y. Li, W. Li, D. Hu, T. Lei, P. Shen, J. Li, S. Gao, Metabolomics analysis reveals the role of cyanidin metabolism in *Plumbago auriculata* flower color, J. Plant Biol. 64 (2021) 253–265, https://doi.org/10.1007/s12374-021-09305-6.
[58] G. Diretto, X. Jin, T. Capell, C. Zhu, L. Gomez-Gomez, Differential accumulation of pelargonidin glycosides in petals at three different developmental stages of the orange-flowered gentian (*Gentiana lutea* L. var. *aurantiaca*), PLoS One 14 (2) (2019) e0212062, https://doi.org/10.1371/journal.pone.0212062.
[59] Z. Zhang, W. Huang, L. Zhao, L. Xiao, H. Huang, Integrated metabolome and transcriptome reveals the mechanism of the flower coloration in cashew *Anacardium occidentale*, Sci. Hortic. 324 (2024) 112617, https://doi.org/10.1016/j.scienta.2023.112617.
[60] W.H. Chen, C.Y. Hsu, H.Y. Cheng, H. Chang, H.H. Chen, M.J. Ger, Downregulation of putative UDP-glucose: flavonoid 3-O-glucosyltransferase gene alters flower coloring in *Phalaenopsis*, Plant Cell Rep. 30 (2011) 1007–1017, https://doi.org/10.1007/s00299-011-1006-1.
[61] M. Gómez-Míguez, S. González-Manzano, M.T. Escribano-Bailón, F.J. Heredia, C. Santos-Buelga, Influence of different phenolic copigments on the color of malvidin 3-glucoside, J. Agric. Food Chem. 54 (15) (2006) 5422–5429, https://doi.org/10.1021/jf0604586.
[62] X. Fu, Q. Wu, J. Wang, Y. Chen, G. Zhu, Z. Zhu, Spectral characteristic, storage stability and antioxidant properties of anthocyanin extracts from flowers of butterfly pea (*Clitoria ternatea* L.), Molecules 26 (22) (2021) 7000, https://doi.org/10.3390/molecules26227000.
[63] J. Zhang, X. Zou, X. Zhai, X. Huang, C. Jiang, M. Holmes, Preparation of an intelligent pH film based on biodegradable polymers and roselle anthocyanins for monitoring pork freshness, Food Chem. 272 (2019) 306–312, https://doi.org/10.1016/j.foodchem.2018.08.041.
[64] D. Sousa, N. Basílio, J. Oliveira, V. de Freitas, F. Pina, A new insight into the degradation of anthocyanins: reversible versus the irreversible chemical processes, J. Agric. Food Chem. 70 (2022) 656–668, https://doi.org/10.1021/acs.jafc.1c05927.
[65] H. Eghbaljoo, M. Alizadeh Sani, I.K. Sani, S.M. Maragheh, D.K. Sain, Z.H. Jawhar, S.M. Jafari, Desenvolvimento de filmes halocrômicos para embalagens inteligentes incorporados com pigmentos de antocianina; avanços recentes, Crit. Rev. Food Sci. Nutr. 65 (2025) 770–786, https://doi.org/10.1080/10408398.2023.2280769.

[66] J. Yan, R. Cui, Y. Qin, L. Li, M. Yuan, A pH indicator film based on chitosan and butterfly pudding extract for monitoring fish freshness, Int. J. Biol. Macromol. 177 (2021) 328–336, https://doi.org/10.1016/j.ijbiomac.2021.02.137.
[67] L. Zhao, Y. Liu, L. Zhao, Y. Wang, Anthocyanin-based pH-sensitive smart packaging films for monitoring food freshness, J. Agric. Food Res. 9 (2022) 100340, https://doi.org/10.1016/j.jafr.2022.100340.
[68] B.S. Nayak, L.M. Pinto Pereira, *Catharanthus roseus* flower extract has wound-healing activity in Sprague Dawley rats, *BMC Complement.* Altern. Med. 6 (1) (2006) 41, https://doi.org/10.1186/1472-6882-6-41.
[69] V.R. Vutukuri, M.C. Das, M. Reddy, S. Prabodh, P. Sunethri, Evaluation of acute oral toxicity of ethanol leaves extract of *Catharanthus roseus* in Wistar albino rats, J. Clin. Diagn. Res. 11 (3) (2017), https://doi.org/10.7860/JCDR/2017/24937.9325.
[70] L. Yuan, M. Gao, H. Xiang, Z. Zhou, D. Yu, R. Yan, A biomass-based colorimetric sulfur dioxide gas sensor for smart packaging, ACS Nano 17 (7) (2023) 6849–6856, https://doi.org/10.1021/acsnano.3c00530.
[71] J. Zhang, J. Zhang, X. Huang, J. Shi, L. Liu, W. Song, M. Povey, A visual bi-layer sensor based on agar/TiO_2/butterfly bean flower anthocyanin/κ-carrageenan with photostability for monitoring *Penaeus chinensis*freshness, Int. J. Biol. Macromol. 235 (2023) 123706, https://doi.org/10.1016/j.ijbiomac.2023.123706.
[72] L. Qiu, M. Zhang, M. Huang, B. Chitrakar, L. Chang, Fabrication of sodium alginate/apricot peel pectin films incorporated with rose anthocyanin-rich extract for monitoring grass carp (*Ctenopharyngodon idellus*) freshness, Food Packag. Shelf Life 39 (2023) 101150, https://doi.org/10.1016/j.fpsl.2023.101150.
[73] O. Romruen, P. Kaewprachu, S. Sai-Ut, et al., Impact of environmental storage conditions on properties and stability of a smart bilayer film, Sci. Rep. 14 (2024) 23038, https://doi.org/10.1038/s41598-024-74004-4.
[74] G. Marappan, H.E. Tahir, N. Karim, A. Lakshmanan, M.R.I. Shishir, S.B. H. Hashim, X. Zou, Natural pigment-based pH/gas-sensitive intelligent packaging film for freshness monitoring of meat and seafood: influencing factors, technological advances, and future perspectives, Food Rev. Int. (2025) 1–38, https://doi.org/10.1080/87559129.2025.2473026.
[75] X. Liu, X. Song, D. Gou, H. Li, L. Jiang, M. Yuan, M. Yuan, A polylactide based multifunctional hydrophobic film for tracking evaluation and maintaining beef freshness by an electrospinning technique, Food Chem. 428 (2023) 136784, https://doi.org/10.1016/j.foodchem.2023.136784.
[76] M. Shayan, J. Gwon, M.S. Koo, D. Lee, A. Adhikari, Q. Wu, pH-responsive cellulose nanomaterial films containing anthocyanins for intelligent and active food packaging applications, Cellulose 29 (18) (2022) 9731–9751, https://doi.org/10.1007/s10570-022-04855-5.
[77] Z. Xiao, L. Han, M. Gu, Y. Zhu, Y. Zhang, Z. Li, F. Lu, Performance comparison of anthocyanin-based smart indicator films, Food Packag. Shelf Life 40 (2023) 101187, https://doi.org/10.1016/j.fpsl.2023.101187.
[78] M. Alizadeh-Sani, M. Tavassoli, E. Maometano, A. Ehsani, G.J. Khaniki, R. Priyadarshi, J.W. Rhim, Filmes indicadores de cor responsivos ao pH à base de nanofibra de metilcelulose/quitosana e antocianinas de bérberis para monitoramento em tempo real do frescor da carne, Int. J. Biol. Macromol. (2020), https://doi.org/10.1016/j.ijbiomac.2020.10.231.
[79] T. Gasti, S. Dixit, O.J. D'souza, V.D. Hiremani, S.K. Vootla, S.P. Masti, R. B. Malabadi, Chitosan/methylcellulose-based smart biodegradable films containing anthocyanin *Phyllanthus reticulatus* for monitoring fish fillet freshness, Int. J. Biol. Macromol. 187 (2021) 451–461, https://doi.org/10.1016/j.ijbiomac.2021.07.128.
[80] H.J. Kim, S. Roy, J.W. Rhim, Gelatin/agar-based color-indicator film integrated with *Clitoria ternatea* flower anthocyanin and zinc oxide nanoparticles for monitoring freshness of shrimp, Food Hydrocoll. 124 (2022) 107294, https://doi.org/10.1016/j.foodhyd.2021.107294.
[81] L.T. Wu, I.L. Tsai, Y.C. Ho, Y.H. Hang, C. Lin, M.L. Tsai, F.L. Mi, Active and intelligent gellan gum-based packaging films for controlling anthocyanins release and monitoring food freshness, Carbohydr. Polym. 254 (2021) 117410, https://doi.org/10.1016/j.carbpol.2020.117410.
[82] J. Coates, Interpretation of infrared spectra, a practical approach, Encycl. Anal. Chem. 12 (2000) 10815–10837.
[83] C.I.L.F. Arias, C. González-Martínez, A. Chiralt, Biodegradation behavior of poly (3-hydroxybutyrate-co-3-hydroxyvalerate) containing phenolic compounds in seawater in laboratory testing conditions, Sci. Total Environ. 944 (2024) 173920, https://doi.org/10.1016/j.scitotenv.2024.173920.
[84] B. Zhu, Y. Zhong, D. Wang, Y. Deng, Active and intelligent biodegradable packaging based on anthocyanins for preserving and monitoring protein-rich foods, Foods 12 (24) (2023) 4491, https://doi.org/10.3390/foods12244491.
[85] R.A. Arumsari, P. Wongphan, N. Harnkarnsujarit, Biodegradable TPS/PBAT blown films with ascorbyl palmitate and sodium ascorbyl phosphate as antioxidant packaging, Polymers 16 (23) (2024) 3237, https://doi.org/10.3390/polym16233237.
[86] N. Piñeros-Guerrero, Y. Piñeros-Castro, R. Ortega-Toro, Active biodegradable films based on thermoplastic starch and poly(ε-caprolactone): technological application of antioxidant extracts from rice husk, Rev. Mex. Ing. Quím. 19 (3) (2020) 1095–1101, https://doi.org/10.24275/rmiq/Poli898.
[87] Y. Amaregouda, K. Kamanna, T. Gasti, Fabrication of intelligent/active films based on chitosan/polyvinyl alcohol matrices containing *Jacaranda cuspidifolia* anthocyanin for real-time monitoring of fish freshness, Int. J. Biol. Macromol. 218 (2022) 799–815, https://doi.org/10.1016/j.ijbiomac.2022.07.174.
[88] M.S. Rabello, Structure and properties of polymers, in: Structure of Crystalline Polymers (Chapter 4), 1st ed, 2021.
[89] K.E. Nissen, B.H. Stuart, M.G. Stevens, A.T. Baker, The tensile and tear properties of a biodegradable polyester film, Int. J. Polym. Anal. Charact. 13 (3) (2008) 190–199, https://doi.org/10.1080/10236660802070538.
[90] K. Akhila, A. Sultana, D. Ramakanth, K.K. Gaikwad, Monitoring freshness of chicken using intelligent pH indicator packaging film composed of polyvinyl alcohol/guar gum integrated with *Ipomoea coccinea* extract, Food Biosci. (2023) 102397, https://doi.org/10.1016/j.fbio.2023.102397.
[91] P.A. Freitas, C. González-Martínez, A. Chiralt, Antioxidant starch composite films containing rice straw extract and cellulose fibres, Food Chem. 400 (2023) 134073, https://doi.org/10.1016/j.foodchem.2022.134073.
[92] F. Shahidi, P. Ambigaipalan, Phenolics and polyphenolics in foods, beverages and spices: antioxidant activity and health effects–a review, J. Funct. Foods 18 (2015) 820–897, https://doi.org/10.1016/j.jff.2015.06.018.
[93] I. Biskup, I. Golonka, Z. Sroka, A. Gamian, Antioxidant activity of selected phenols estimated by ABTS and FRAP methods, Adv. Hyg. Exp. Med. 67 (2013) 958–963.
[94] S. Roy, H.J. Kim, J.W. Rhim, Effect of blended colorants of anthocyanin and shikonin on carboxymethyl cellulose/agar-based smart packaging film, Int. J. Biol. Macromol. 183 (2021) 305–315, https://doi.org/10.1016/j.ijbiomac.2021.04.162.
[95] K.P. Chaithra, T.P. Vinod, P. Nagarajan, Smartphone application-based colorimetric fish freshness monitoring using an indicator prepared by rub-coating of red cabbage on paper substrates, Colloids Surf. A Physicochem. Eng. Asp. 679 (2023) 132553, https://doi.org/10.1016/j.colsurfa.2023.132553.
[96] B. Kuswandi, A. Jayus, A. Restyana, A. Abdullah, L.Y. Heng, M. Ahmad, A novel colorimetric food package label for fish spoilage based on polyaniline film, Food Control 25 (2012) 184–189, https://doi.org/10.1016/j.foodcont.2011.10.008.
[97] W. Mokrzycki, M. Tatol, Colour difference ΔE – a survey, Mach. Graph. Vis. 20 (2011) 1–28.
[98] M. Rusishvili, L. Grisanti, S. Laporte, M. Micciarelli, M. Rosa, R.J. Robbins, T. Collins, A. Magistrato, S. Baroni, Unraveling the molecular mechanisms of color expression in anthocyanins, Phys. Chem. Chem. Phys. 21 (2019) 8757–8766, https://doi.org/10.1039/C9CP00747D.
[99] K. Sakata, N. Saito, T. Honda, Ab initio study of molecular structures and excited states in anthocyanidins, Tetrahedron 62 (2006) 3721–3731.
[100] M.A. Sani, M. Tavassoli, H. Hamishehkar, D.J. McClements, Carbohydrate-based films containing pH-sensitive red barberry anthocyanins: application as biodegradable smart food packaging materials, Carbohydr. Polym. 255 (2021) 117488, https://doi.org/10.1016/j.carbpol.2020.117488.
[101] N. Fallah, A. Aarabi, H. Zaki Dizaji, M. Ghashang, Development of a colorimetric intelligent film based on biodegradable polymers incorporated with *Hibiscus sabdariffa* anthocyanins for monitoring salmon fish spoilage, Food Bioprocess Technol. (2025) 1–17, https://doi.org/10.1007/s11947-024-03713-5.
[102] K.A. Oduse, T. Makinde, A. Saini, R.T. Alves, V.L. Reta, B.M. Tello, Development of intelligent packaging for real-time monitoring of the freshness of Canadian fish (tilapia and salmon) and pork during storage, Int. Food Res. J. 32 (1) (2025) 186–194, https://doi.org/10.47836/ifrj.32.1.13.
[103] C. Shi, J. Zhang, Z. Jia, X. Yang, Z. Zhou, Intelligent pH indicator films containing anthocyanins extracted from blueberry peel for monitoring tilapia fillet freshness, J. Sci. Food Agric. 101 (5) (2021) 1800–1811, https://doi.org/10.1002/jsfa.10794.
[104] Y. Yang, X. Yu, Y. Zhu, Y. Zeng, C. Fang, Y. Liu, S. Hu, Y. Ge, W. Jiang, Preparation and application of a colorimetric film based on sodium alginate/sodium carboxymethyl cellulose incorporated with rose anthocyanins, Food Chem. 393 (2022) 133342, https://doi.org/10.1016/j.foodchem.2022.133342.
[105] N.S. Said, N.M. Sarbon, Monitoring the freshness of fish fillets by colorimetric gelatin composite film incorporated with curcumin extract, Biocatal. Agric. Biotechnol. 50 (2023) 102722, https://doi.org/10.1016/j.bcab.2023.102722.
[106] T.A. Misharina, M.B. Terenina, N.I. Krikunova, Antioxidant properties of essential oils, Prikl. Biokhim. Mikrobiol. 45 (2009) 710–716, https://doi.org/10.1134/S0003683809060175.